Ozone Chemically-Enhanced Backwashes For Ceramic Membrane Fouling Control in Cyanobacteria-Laden Surface Water Applications

by

Stéphane Venne

A thesis submitted to the Faculty of Graduate and Postdoctoral Affairs
in partial fulfillment of the requirements of the degree of

Master of Applied Science

in

Environmental Engineering

Carleton University
Ottawa, Ontario

Abstract

Membranes have been shown to be effective physical barriers against cyanobacteria, however, membrane fouling in surface waters impacted by cyanobacteria is poorly controlled and results in high operating costs. A possible solution is the chemically-enhanced backwash (CEB), a cleaning strategy in which a chemical is combined with a hydraulic backwash for *in-situ* fouling control. This research investigates the potential of using an ozone CEB to control the fouling caused by *Microcystis aeruginosa* in surface water on a ceramic ultrafiltration membrane. To this end, batch ozonation tests and dead-end, continuous flow, experiments were conducted with ozone doses between 0 and 19 mg O_3/mg carbon on the membrane. Water samples used in theses experiments were partially-treated surface water, cyanobacteria-spiked ultrapure water, and cyanobacteria-spiked partially-treated surface water. In the batch tests, ozone reacted more rapidly with the surface water foulants than with cyanobacteria. Interestingly, the opposite was observed during a CEB, highlighting the contribution of the hydraulic force to the cleaning effects of a CEB. Ozone likely weakens the highly compressible cake layer formed by cyanobacteria on the membrane surface during filtration, which is then more hydraulically reversible. This became clearer when operating the membrane over several filtration cycles. In fact, the first CEB offered a slight improvement over the traditional hydraulic backwash but the second CEB, which was initiated once more cyanobacteria accumulated on the membrane,

reduced the fouling resistance by 48.5% more than the hydraulic backwash. Overall, all ozone CEBs over two filtration cycles were capable of recovering over 80% of the membrane's specific flux whereas only 66% overall was recovered without the use of ozone.

Acknowledgements

Firstly, I would like to thank my two supervisors: Dr. Onita Basu and Dr. Benoit Barbeau. Their guidance and unwavering optimism throughout all stages of this research was motivating and much appreciated. I am very grateful for the opportunities that were given to me. As a whole, this project was a great learning experience and has helped shape my career path.

À la Polytechnique de Montréal, j'aimerais remercier l'équipe de techniciens du CREDEAU: Yves Fontaine, Mireille Blais, Jacinthe Mailly, Julie Philibert, Gabriel St-Jean et Tetiana Elyart pour leur expertise technique. Leur présence quotidienne a rendu les travaux de laboratoire très agréables.

In Ottawa, I would like to thank Marie Tudoret and Richard Kibbee for their help with the growth of cyanobacteria. Also, a special thank you to all my colleagues, class, lab, and office mates for their support and for making the two years of my degree a very enjoyable experience.

Finalement, le tout n'aurait pas été possible sans l'encouragement continu de ma famille: mon père Marc, ma mère Danielle et mon frère Joël Venne.

Encore une fois, merci à tous.

Contents

List of Tables

List of Figures

List of Acronyms

CEB Chemically-enhanced backwash

CIP Clean-in-place

Cyano-UW Cyanobacteria-spiked ultrapure water

Cyano-SW Cyanobacteria-spiked surface water

DOC Dissolved organic carbon

FEEM Fluorescence Excitation-Emission Matrix

NOM Natural organic matter

SW Surface water

TOC Total organic carbon

Chapter 1

Introduction

1.1 Problem statement

Cyanobacteria, also known as blue-green algae, are prokaryotic microorganisms (O'Neil et al., 2012) naturally found in the phytoplankton communities of freshwater and marine ecosystems (G. Hairston Jr. and Fussmann, 2017). Similar to other planktonic species, cyanobacteria form blooms during the temperate seasons (Pick, 2016). Generally, these blooms, which are large accumulations of biomass, are considered harmful as they are potentially toxic. They negatively impact both the water body's ecosystem and produced drinking water quality, which in turn threatens human health (WHO, 2017). Given that the growth of cyanobacteria has accelerated in the last two decades, harmful blooms have become more frequent, more intense, longer in duration, and consequently, have become a subject of urgent concern (O'Neil et al., 2012).

In North America specifically, harmful blooms are reported frequently in the public media and are often identified on Lake Champlain, Lake Ontario, Lake Winnipeg, and Lake Erie (Pick, 2016). For example, since 2008, a significant harmful bloom

dominated by the *Microcystis aeruginosa* cyanobacterium forms almost annually in Lake Erie, as seen in figure 1.1 (NOAA, 2019).

At the source of the problem, it is believed that the nutrient runoff from anthropogenic activities is one of the primary drivers of cyanobacteria's accelerated growth since this growth is controlled by the availability of phosphorus (O'Neil et al., 2012). Regulations such as the Great Lakes Water Quality Agreement effectively decreased the total phosphorus loading in the Great Lakes but the onset of climate change threatens to perpetuate and even worsen the proliferation of cyanobacteria (C. Ho and Michalak, 2015; Pick, 2016). More specifically, the concomitant changes in atmospheric carbon dioxide levels as well as in the surface water's temperature, column stratification, and pH create conditions under which cyanobacteria thrive (O'Neil et al., 2012).

As for drinking water production, the impacts of the Lake Erie bloom were made clear in 2014, when the toxicity of the bloom forced the community of Toledo (Ohio) to impose a three-day water ban, limiting a half-million residents' access to drinking water (C. Ho and Michalak, 2015). This toxicity originates from the capability of cyanobacteria to produce secondary metabolites (Campinas and Rosa, 2010), which are mostly hepatotoxins and neurotoxins. Some are only produced by a number of cyanobacteria species, such as microcystins and anatoxin-a, whereas others can be produced by all species, such as β-methylamino-L-alanine (O'Neil et al., 2012). Most of these can be contained within the cyanobacteria cells (intracellular). For this reason, the World Health Organization (WHO) has recommended that treatment focuses on removing cells whole, thus limiting the release of toxins in the water matrix. Additionally, the WHO has recommended that the total microcystin-LR toxin limit be set to 1 μg/L (WHO, 2017). However, treating water affected by cyanobacteria blooms is complicated by the difficulties associated with predicting bloom formation

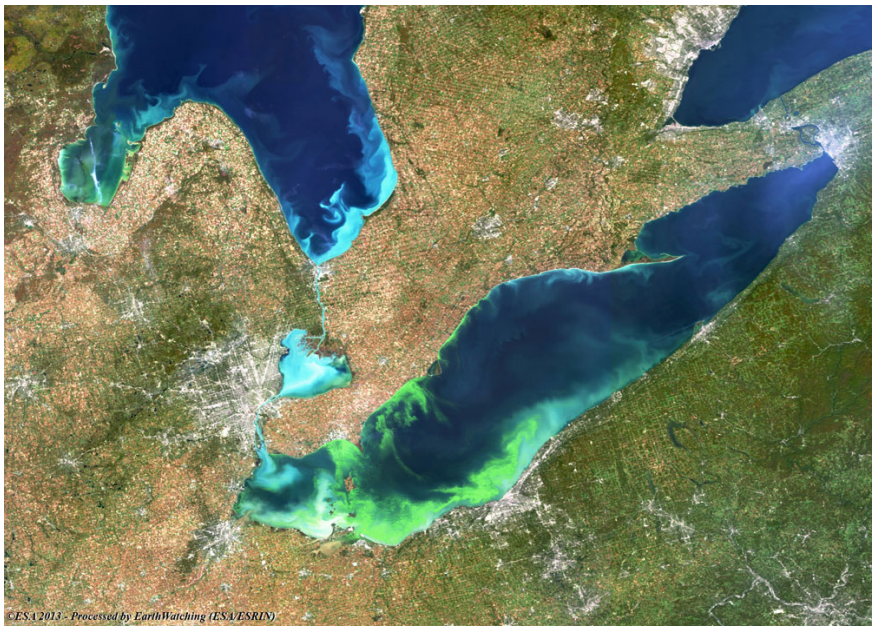

(a)

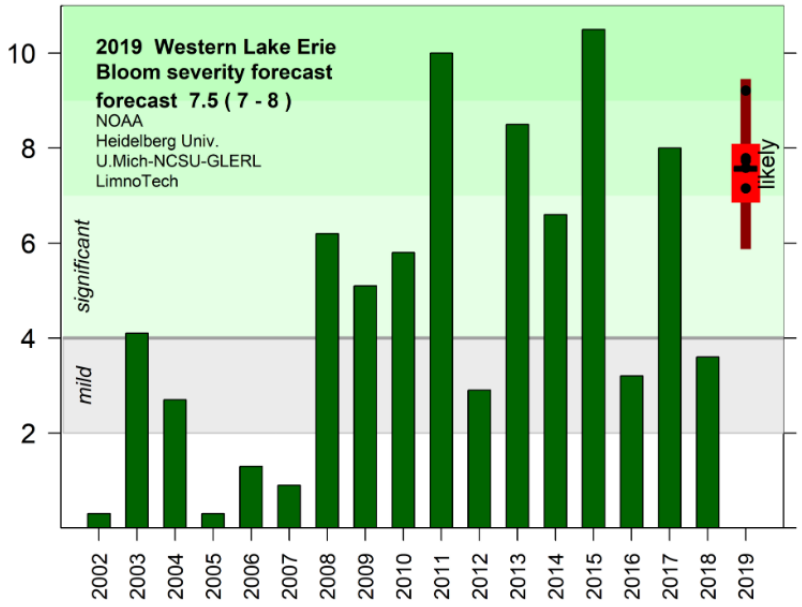

(b)

Figure 1.1: a) Satellite image of the harmful bloom in the western basin of Lake Erie taken on October 8, 2011 (ESA, 2019). b) Severity of harmful algal blooms in Lake Erie over the years. The y-axis represents the bloom's severity index and is determined by the bloom's biomass and its duration (NOAA, 2019). This year, the bloom on Lake Erie was actually ranked as the fifth largest since 2002 (Taylor, 2019).

and bloom toxicity. More precisely, blooms cannot be solely identified by the presence of surface scum (Pick, 2016). Also, on average, 59% of worldwide bloom events are toxic (USEPA, 2019) but a correlation doesn't necessarily exist between a bloom's size and its toxicity (NOAA, 2019).

Overall, blooms pose difficult challenges to drinking water treatment plants, which were not designed to adapt to large and rapid changes in cyanobacteria cell concentrations and toxicity. In conventional treatment plants, these changes result in the application of inadequate chemical dose during coagulation. Also, since cyanobacteria cells have a tendency to float, breakthrough of cells can be observed in settled water. This can create taste and odour issues while also increasing water turbidity and the formation of disinfection by-products, possibly resulting in the loss of regulatory compliance for finished water quality (Coral et al., 2013). For instance, Zamyadi et al. (2012) demonstrated that due to large daily fluctuations of cyanobacteria cell concentrations and toxicity, as much as 3% of cyanobacteria cells and toxins actually broke through to finished water at the drinking water treatment plant located at the Missisquoi Bay of Lake Champlain, even after chlorine disinfection.

These performance issues encountered in conventional treatment processes prompts the need for the development of treatment solutions that are both effective and sustainable in terms of cost, energy, resources, and applicability (Lieu Le and Nunes, 2016). Meanwhile, low-pressure ultrafiltration membranes have been shown to completely remove even the smallest cyanobacteria cells from water (*M. aeruginosa*, 3-10 μm) by size exclusion and with minimal toxin release (Campinas and Rosa, 2010). Presently, the biggest limitation of membrane technology is the rapid decrease in performance caused by fouling, increasing operational costs and shortening a membrane's useful life. Fouling is a process by which contaminants accumulate on a membrane's surface and within its pore structure (Gao et al., 2011). In the event of a harm-

ful bloom, the greatest contributors to membrane fouling are cyanobacteria cells (Qu et al., 2012a; Liu et al., 2017) and the natural organic matter (NOM) in surface water (Hofs et al., 2011; Xia et al., 2013).

It is possible to control fouling either by mitigation techniques such as feed pretreatment or by alleviation techniques such as physical and chemical cleaning. In membrane filtration processes, a simple physical cleaning strategy, known as a hydraulic backwash, is periodically executed to remove fouling and requires only that the flow of water through the membrane be reversed for a short period of time (seconds to a few minutes). Since a fraction of the fouling remains on the membrane, an aggressive chemical wash is eventually necessary to remove this physically irreversible fraction of fouling. Chemical cleaning is most commonly achieved with a clean-in-place (CIP) operation, which requires that the membrane be soaked in chemicals for extended periods of time (several hours to half a day). The drawbacks of a CIP are that it requires process adjustments, requires large chemical concentrations, and results in costly downtime (Shi et al., 2014). A chemically-enhanced backwash (CEB) is an alternative strategy in which a chemical, at a relatively small concentration, is combined with a hydraulic backwash for an *in-situ* cleaning process that requires no downtime (Chang et al., 2017).

In drinking water treatment, chlorine is the mostly used chemical in CIP and CEB procedures. However, the application of this oxidant in a CEB results in the formation of undesirable trihalomethanes and halogens in water with high organic content, such as surface water dominated by cyanobacteria blooms. There are also concerns that frequent chlorine applications will cause the formation of carbonate scale in the membrane module, a type of fouling that must be removed by an acid CIP at low pH (≤ 2) (Chang et al., 2017).

One potential alternative to chlorine is ozone. Ozone is of particular interest

for CEB applications as it reacts more rapidly than chlorine with organic material in water (Van Geluwe et al., 2011) and smaller exposures (as small as 0.2 mg·min/L) can fatally damage cyanobacterial cells (Coral et al., 2013). Furthermore, the catalytic decomposition of ozone by ceramic materials leads to the formation of stronger and less selective oxidants, making the combination of ozone and ceramic membranes very attractive and yielding new opportunities for membrane fouling control (Van Geluwe et al., 2011). In comparison, polymeric membranes, which are presently more widely used in water treatment plants due to their lower capital cost (Chang et al., 2017), are actually damaged by repeated exposure with oxidants (Gao et al., 2011). This results in the need for more frequent membrane replacements.

The use of ozone in a CIP was previously studied by Alresheedi et al. (2019) to clean a ceramic membrane fouled by natural organic matter. The authors noted that the ozone CIP was able to achieve the same degree of cleaning as a chlorine CIP in a quarter of the time. When cyanobacteria cells are present in the water, Wei et al. (2016) noted that that the continuous addition of ozone to the membrane influent could reduce the accumulation of fouling on the membrane by approximately 76%. Although these ozone applications are improvements on the chlorine CIP, they remain costly. More specifically, an ozone CIP still requires process interruptions (Alresheedi et al., 2019) and feed pre-ozonation requires the continuous addition of ozone, possibly affecting permeate quality and requiring additional post-membrane treatment (Xia et al., 2013).

An ozone chemically-enhanced backwash addresses both the issues of the ozone CIP and feed pre-treatment. In a CEB application, the membrane is only intermittently exposed to ozone, that is, only during the CEB. Consequently, less ozone is consumed than when ozone is continuously added to the feed (as in pre-treatment applications). Also, oxidized foulants are less likely to accumulate in the permeate

as they are discharged with the CEB effluent. Yet, the ozone CEB is poorly understood in literature. Most studies discussing CEB applications apply a chlorine CEB for membrane fouling control in seawater desalination and feed water that has a low particulate organic matter concentration. Additionally, the CEB is rarely the primary focus of these studies, which generally address the application of low-pressure membranes as a pre-treatment step to reverse osmosis. The frequency of the CEB and the oxidant dose varies greatly between studies (between every 1 to 24 hours; 1 to 500 mg/L Cl_2) and appears to be chosen arbitrarily. Although the chlorine CEB was capable of reducing the need for a CIP and in some cases, maintain the membrane's clean specific flux, there appears to be opportunities for the optimization of these operational parameters (Chang et al., 2017). On the other hand, the application of an ozone CEB in wastewater treatment was shown to recover over 99% of the membrane productivity (Fujioka and Nghiem, 2015). Once again, the impact of ozone dose, mechanisms of foulant removal, and the kinetics of foulant removal were not discussed in detail. As for the use of a CEB to control membrane fouling in surface waters impacted by cyanobacterial blooms, no previous studies were found.

1.2 Research objectives

The main objective of this research is to demonstrate the potential of ozone chemically-enhanced backwashes to control the fouling of ceramic ultrafiltration membranes exposed to cyanobacteria and natural organic matter in surface water. Furthermore, this research seeks to understand the cleaning kinetics and mechanisms involved in the process, which will help develop the fundamental understanding required to optimize the application of ozone chemically-enhanced backwashes. From a general perspective, this research will help highlight the potential of ceramic membranes for drinking

water treatment.

1.2.1 Specific objectives

The general objective of this research is supported by the following specific objectives, which are to:

1. Determine the role of ozone in a CEB by comparing its performance to the performance of a hydraulic (water-only) backwash when cleaning a membrane fouled by real surface water and cyanobacteria;

2. Determine the rate of ozone demand and the rate of organic foulant removal from the membrane during an ozone CEB, and;

3. Evaluate the effect of ozone dose on foulant removal and on membrane productivity.

1.2.2 Hypotheses

Based on the limited CEB literature, it is hypothesised that:

1. During a CEB, ozone alleviates hydraulically irreversible fouling but has no impact on fouling between chemically-enhanced backwashes;

2. Ozone demand during a CEB is a predictor of foulant removal and of cleaning performance, and;

3. A larger ozone dose results in a greater foulant removal and improved membrane productivity.

1.3 Thesis structure

This thesis is separated into 5 chapters, as follows:

Chapter 1 introduces the motivation behind the research, summarizing the need for it from a real-life and scientific perspective. In this chapter, the general and specific objectives are also listed.

Chapter 2 presents a review of membranes processes and the current state of research in the field of membrane fouling and cleaning. The focus of the review is mainly on fouling by surface water and by cyanobacteria as well as on the previously studied ozone and ceramic membrane cleaning applications.

Chapter 3 is a detailed description and justification of the materials and methods used in the experimental design.

Chapter 4: Ozone chemically-enhanced backwash for the control of ceramic membrane fouling by cyanobacteria *(Planned submission to Journal of Membrane Science)*

Authors: Stéphane Venne, Onita Basu, Benoit Barbeau

Author contributions:

- Stéphane Venne: Performed all the experiments, which included modifying the membrane system, sampling the surface water, preparing the cyanobacteria cultures, and collecting data. Analyzed the data, developed all tables and figures, and wrote the paper in full.

- Onita Basu: Thesis co-supervisor. Developed the experimental design. Provided guidance and feedback throughout all stages of the research. Reviewed the data analysis, reviewed the article drafts, and recommended edits throughout the writing stage.

- Benoit Barbeau: Thesis co-supervisor. Developed the experimental design. Provided guidance and feedback throughout all stages of the research. Reviewed the data analysis, reviewed the article drafts, and also recommended edits.

Chapter 5 summarizes the results and conclusions obtained in this research, which are compared to the research objectives listed in chapter 1. The opportunities for future work are briefly discussed.

Chapter 2

Literature review

Membrane filtration has become an increasingly attractive technology in the field of drinking water treatment given its numerous advantages over and in conjunction with conventional coagulation, sedimentation and filtration treatment mechanisms. Overall, membranes can reliably produce high quality water as their performance is mostly independent of variations in feed water characteristics and upstream chemical dosage. They also provide an ultimate barrier against bacteria and, in some cases, viruses (Pearce, 2007). This improved performance is becoming especially advantageous as concerns of emerging contaminants, such as cyanobacteria, are multiplying. Membrane fouling, defined as the accumulation of contaminants on the membrane surface or within its pore structure (Huang et al., 2008; Gao et al., 2011), still limits its widespread application in drinking water treatment plants and drastically increases operating costs. Fouling causes the decrease of membrane permeability, observed as either an increase in operating pressure or a decrease in water flux.

In order to properly design and evaluate the use of an ozone CEB for the cleaning of a ceramic membrane fouled by surface water and cyanobacteria, an understanding of membrane processes, of the nature of these foulants, of membrane fouling mechanisms,

and of previously studied cleaning strategies is imperative.

2.1 Principles of membrane filtration in drinking water treatment

Membrane filtration is a pressure-driven process in which contaminants can be separated from water by size exclusion (Gao et al., 2011). More specifically, the membrane's porous structure acts as a physical barrier to foulants that are larger than the membrane's nominal pore size. Contaminants smaller than the pores can also be removed via specific and non-specific interactions with the membrane material but in most cases, this removal is limited by the membrane's adsorptive capacity. Consequently, considerations for the membrane's pore size and material are crucial when selecting a membrane as it directly impacts the rejection of contaminants, the membrane's permeability, the operating pressure, and therefore, membrane fouling as well as operating costs (Van der Bruggen et al., 2003).

Based on the pore sizes, membrane processes can be generally categorized as listed in table 2.1. It is worth noting that, in some cases, the membrane pore size or its rejection capacity can alternatively be expressed in terms of molecular weight cut-off (MWCO), defined as the molecular weight at and above which 90% of contaminants are removed by the membrane (Van der Bruggen et al., 2003).

Of the four membrane processes, microfiltration and ultrafiltration applications are considered to be low-pressure processes. Both types of applications are preferred for the production of drinking water from freshwater and both types of membrane were shown to be effective for the removal of cyanobacteria cells in water (Babel and Takizawa, 2011). Depending on the treatment objectives, using ultrafiltration

Table 2.1: Classification of membrane processes and associated operational parameters. Adapted from Van der Bruggen et al. (2003)

Parameter	Microfiltration (MF)	Ultrafiltration (UF)	Nanofiltration (NF)	Reverse osmosis (RO)
Pore size (nm)	100 - 10000	2 - 100	0.5 - 2	< 0.5
Rejects	Particles (ex.: bacteria)	Same as MF + macro-molecules and viruses	Same as UF + multivalent ions and dissolved organics	Same as NF + monovalent ions
Permeability (LMH/bar)	> 1000	10 - 1000	1.5 - 30	0.05 - 1.5
Operating pressure (bar)	0.1 - 2	0.1 - 5	3 - 20	5 - 120

membranes can be advantageous as they can remove viruses and a fraction of the natural organic matter found in surface water (Campinas and Rosa, 2010). It is worth noting that the majority of full-scale drinking water treatment plants that use membranes operate them in dead-end filtration with at a constant flux (Huang et al., 2008). During dead-end filtration, the flow of water is perpendicular to the membrane and all of the feed influent is forced through the membrane, becoming the permeate. An alternative configuration is cross-flow filtration, in which water flows tangentially to the membrane surface and a portion of the water does not pass through the membrane and carries foulants away from the membrane surface. This stream is known as the retentate or concentrate. Typically, dead-end filtration is preferred as process equipment required is simpler and water losses are minimalized (Van der Bruggen et al., 2003).

In regard to the selection of membrane materials, polymeric membranes are the most widely used in drinking water treatment. Their popularity is also reflected in the literature on low-pressure membranes (MF/UF), where polymeric membranes are currently used in 88.4% of studies (Chang et al., 2017). In comparison, ceramic membranes can offer several advantages over their polymeric counterparts, despite their higher capital cost. This includes their greater mechanical strength, their greater chemical and thermal stability, their improved hydrophilicity, and their narrower pore size distribution (Amin et al., 2016). These properties can help minimize fouling and allow treatment plants to make use of more aggressive cleaning solutions (such as dissolved ozone solutions) without damaging the membranes (Amin et al., 2016). Moreover, ozone is of particular interest since ceramic materials such as titanium dioxide (TiO_2), zirconium dioxide (ZrO_2), and aluminum oxide (α-Al_2O_3) have been shown to act as catalysts, promoting the formation of highly reactive radicals. Ozone and radical chemistry will be discussed in greater detail in section 2.4.

Although a membrane's properties and operational conditions are important factors to consider when limiting fouling, attention is also required for the feed water characteristics as they have been shown to have the greatest impact on fouling. For instance, the normalized specific flux decline in a membrane system varied by more than 25% when the treated surface water source was changed (4 different sources tested) whereas it varied by less than 10% when the operating conditions were changed (membrane flux was doubled from 54 to 109 LMH) (Chang et al., 2017).

2.2 Fouling of ultrafiltration membranes

2.2.1 Fouling mechanisms

In low-pressure membrane applications, fouling can be described by a single or a combination of the blocking laws proposed by Hermia (Huang et al., 2008): complete pore blocking, intermediate pore blocking, standard pore blocking, and cake layer formation.

In the complete pore blocking regime, the foulant particles are larger than the pores and consequently, a particle completely obstructs a pore. In this regime, the particles are not deposited on the membrane surface between pores or on other foulants. Intermediate pore blocking is similar except that foulants can adsorb on other particles on the membrane. In the case of cake fouling, the foulants are deposited on the membrane surface between pores and on other foulants. Compared to the pore blocking laws, it is the porous structure of the cake that contributes most to the decrease in membrane performance instead of the physical obstruction of pores. Finally, standard pore blocking occurs when foulants are smaller than the membrane pores and become attached on the internal walls of the pores. This constricts the pores and

effectively reduces their size (Huang et al., 2008).

The adsorption of foulants that takes place in standard pore blocking and the early stages of cake formation is due to Van der Waals forces, electrostatic affinities, or chemical bonding. Adsorption, as well as complete and intermediate pore blocking, will typically be the dominating fouling mechanisms in the early stages of filtration, when a membrane surface is most exposed (i.e. when a new membrane is first put in use or after a membrane was chemically cleaned) (Xia et al., 2013). As time passes, foulants accumulate on the membrane surface and a cake is formed. While the cake blocks the membrane pores to some extent, in some cases this cake can also act as a filter aid and facilitates the removal of other foulants (Shi et al., 2014; Babel and Takizawa, 2011).

In practice, the extent of membrane fouling can be quantified using the resistance-in-series model or fouling indexes, such as the unified-membrane fouling index (UMFI). It is worth noting that the UMFI only applies to incompressible cakes and thus does not apply to compressible cakes (Huang et al., 2008). Generally, fouling can be described as either reversible or irreversible, indicating whether or not it was removed by a membrane cleaning step (Gao et al., 2011). In the discussions to follow, the terms "reversible fouling" and "irreversible fouling" are used to refer to the fractions of fouling that can and cannot be removed by a physical cleaning step (discussed in section 2.3), unless specified otherwise.

2.2.2 Fouling by surface water

Natural organic matter (NOM) describes a large group of carbon-based compounds that can naturally be found in surface water and is thought to be one of the most challenging foulants to control in drinking water treatment. This group of com-

pounds is comprised of carbohydrates, proteins, polysaccharides, and other extracellular macromolecules produced by microorganisms. It also includes humic and fulvic acids produced by the decay of plant and animal residues (Van Geluwe et al., 2011). The complex composition of this mixture makes it difficult to predict its fouling behaviour, especially since NOM can be in particulate, colloidal or dissolved form and its compounds have varying molecular weights and functional groups. Furthermore, the large structure of humic substances, which makes up 80% of total organic carbon in surface water (Shi et al., 2014), is poorly defined (Van Geluwe et al., 2011).

The impacts of the complex composition of NOM on membrane fouling were highlighted in the experiments conducted by Xia et al. (2013). The authors showed that the rejection of a model humic acid by an ultrafiltration ceramic membrane (operated in cross-flow) differed from the rejection of humic substances in real surface water. At various trans-membrane pressures, the removal of the model foulant was always greater than 50% whereas the removal of real surface water NOM was always below 20%. Further analysis suggested that large differences in the molecular size of the humic substances could explain the differences in removal. In a separate study, Hofs et al. (2011) compared the performance of polymeric and ceramic membranes. They showed that a much larger fraction of the NOM fouling was reversible on the ceramic membrane, even though the amount of total fouling was similar on both ceramic and polymeric membranes. It was also shown that the hydrophobic NOM fractions are preferentially retained by the membrane during filtration. It is therefore not surprising that they are also responsible for the majority of irreversible fouling on ceramic membranes (Xia et al., 2013). In comparison, proteins also cause largely irreversible fouling. In fact, since their functional groups are partially hydrophobic, they rapidly and strongly adsorb onto membrane surfaces (Shi et al., 2014).

It should be noted that the presence of other contaminants in the surface water

matrix can have an impact on fouling by NOM. In fact, fouling is believed to be exacerbated by the presence of divalent cationic metals such as calcium and magnesium. They can form complexes with foulants, which reduces the foulants' negative surface charge. This weakens the electrostatic repulsive forces in foulant-foulant interactions as well as in interactions between the foulants and the membrane surface (Qu et al., 2012b). This negative effect was also observed by Alresheedi et al. (2019). Alresheedi et al. (2019) also noted both an increase in fouling index (UMFI) as well as a decrease in the foulant's (alginate) zeta potential when calcium was added to the feed water. Consequently, the foulant interactions are strengthened and a greater fraction of the total fouling is irreversible.

2.2.3 Fouling by cyanobacteria

Membrane fouling by cyanobacteria is governed by several fouling mechanisms given that cyanobacteria-laden water is a heterogeneous mixture of intact cells, cell debris, and dissolved algal organic matter (AOM, which is the sum of intracellular and extracellular organic matter). Liu et al. (2017) compared the fouling potential of these components in water contaminated by *M. aeruginosa* on flat-sheet polyvinylidene fluoride ultrafiltration membranes (60 kDa MWCO, constant pressure filtration). They determined that the cells were responsible for the greatest increase in membrane resistance but that approximately 97% of the resistance caused by the cells was reversible. In contrast, an increase of cell debris and algal organic matter in water increases the fraction of fouling that is irreversible. It is thought that this increase can be explained by the difference in cohesive and adhesive free energies of the foulants. In other words, these energies quantify the foulants' tendency to deposit on other foulants and their tendency to deposit on the membrane surface. Since the free energies of debris and

algal organic matter are negative, they are more likely to adsorb on the membrane surface and to self-agglomerate than cells, which have positive free energies. When cyanobacteria cells and algal organic matter are both present in solution, the free energies of the foulant mixture as a whole is slightly neutralized (Liu et al., 2017).

Qu et al. (2012a) performed similar fouling experiments with *M. aeruginosa* but with flat-sheet polyethersulfone ultrafiltration membranes (100 kDa MWCO, dead-end, constant pressure filtration). They observed that an increase in feed cell concentration from 5.0×10^5 to 4.0×10^6 cells/mL resulted in a dramatic decrease in permeate flux, as expected. For all tested cell concentrations, the irreversible fouling accumulated on the membrane was greater after each physical cleaning step. Interestingly, although the accumulation of reversible fouling was more rapid at a higher cell concentration, the rate of irreversible fouling did not increase. From this observation, it can be concluded that the irreversible fouling was caused in large part by the adsorption of foulants on the membrane surface and within the membrane pores. This adsorption is limited once a foulant cake layer had formed. In other words, higher cell concentrations simply resulted in a thicker cake formation. The fraction of irreversible fouling by cells was small (approximately 16%) but was larger than observed in the study by Liu et al. (2017). Different membrane properties and cell debris in the feed, although not quantified in the study by Qu et al. (2012a), is thought to be the cause of this difference.

Cell debris and algal-derived organic matter can also bind with the cells in the cake layer, decreasing its porosity and increasing the degree of the fouling's irreversibility. Studies suggest that the hydrophobic proteins and polysaccharides in the AOM are the main components that adsorb into the cake layer (Qu et al., 2012a; Babel and Takizawa, 2011) but it is worth noting that the composition and quantity of algal organic matter in the water matrix is dependent of the age of the cyanobacteria cells.

For instance, when filtering 1-month old (start of stationary growth phase) and 3-month old *M. aeruginosa* cultures on ultrafiltration membranes, older cells were more prone to be lysed under the pressure and cross-flow of water (Campinas and Rosa, 2010).

The porosity of the foulant cake layer might also decrease under compressive stresses, once again increasing the fraction of fouling that is irreversible. In their research, both Qu et al. (2012a) and Liu et al. (2017) observed that the cake layer formed by cyanobacteria is compressible, as confirmed by a sharp and exponential increase in trans-membrane pressure, especially at higher cell concentrations. Interestingly, Babel and Takizawa (2011) demonstrated that the cake formed by a natural culture of *Chlorella* algae on two microfiltration membranes (one made of cellulose ester and the other made of modified polyvinylidene difluoride, both with a pore size of 0.45 μm) had a maximum degree of compressibility. In other words, once a pressure threshold was achieved, which is likely specific to every algae species but appears to be independent of the membrane characteristics in their study, the algae cells do not compress further.

2.3 Ultrafiltration membrane fouling control

2.3.1 Feedwater pre-treatment

By partially treating the feed water prior to membrane filtration, it is possible to reduce the quantity of foulants that reach the membrane and to alter the chemical properties of the water, reducing foulant adsorption and increasing fouling reversibility. Pre-treatment methods include coagulation, dissolved air flotation, sand filtration, and oxidation. For instance, Yu et al. (2019) extended the operation time of an

ultrafiltration membrane by a factor of three by using pre-coagulation. Although it was shown that optimized pre-treatment can remove over 95% of cyanobacteria cells in feed water, the large cell concentrations identified in cyanobacterial blooms (sometimes in excess of 1×10^7 cell/mL (Babel and Takizawa, 2011)) effectively means that a relatively large quantity of cells still reach the membrane surface and that the rate of membrane fouling is simply reduced by feed pre-treatment (Liu et al., 2017). Besides, pre-treatment of cyanobacteria cells by oxidation lyses them, releasing their intracellular organics (toxins as well as taste and odour compounds). These can foul membranes irreversibly and deteriorate the quality of the produced water (Coral et al., 2013).

2.3.2 Physical cleaning

Physical cleaning generally consists of reversing the flow of water through the membrane (i.e. water flows from the permeate to the feed side) for a short period of time. This cleaning strategy is known as a hydraulic backwash and its efficiency is dependent on its frequency, duration, and strength. If the filtration time between backwashes is too long, the foulants are compacted on the membrane and become more difficult (i.e. require more energy) to remove, especially if the backwash is too short and too weak to expand and remove the formed foulant cake. In contrast, more frequent, longer, and stronger backwashes are not necessarily advantageous as larger volumes of permeate and greater quantities of energy are required for cleaning, decreasing overall membrane productivity. The water used for the backwashes can also impact cleaning effectiveness. Notably, it was observed that backwashing membranes with deionized water resulted in a smaller accumulation of irreversible fouling during filtration. However, for practical reasons, full-scale membrane applications typically

use permeate for backwash operations (Chang et al., 2017).

Considering these factors, in treatment plants using low-pressure membranes, more than 80% of backwashes are initiated at intervals between 10 and 60 minutes and have a duration of 10 to 90 seconds. Based on observation, the optimal strength of the backwash, which is defined as the ratio of the backwash flux and permeate flux or the ratio of the backwash pressure and feed pressure, is believed to be between 1.5 and 2.5 (Chang et al., 2017).

From a different perspective, physical cleaning of membranes can also be achieved through air scouring and membrane relaxation (De Souza and Basu, 2013). Air scouring involves the removal of foulants from the membrane surface (and to a much lesser extent, from within the pores) by the shear abrasive forces of air bubbles introduced in the membrane module. The air bubbles can be introduced continuously or intermittently, either during filtration or during the hydraulic backwashes (Chang et al., 2017). In contrast, relaxation consists of completely stopping the flow of water through the membrane for a short period of time, during which foulants diffuse away from the membrane due to concentration gradients in solution (Habib et al., 2017). Nonetheless, the effectiveness of physical cleaning generally decreases over time. This is especially true when the physical cleaning steps are initiated at fixed intervals. In those cases, backwashes are likely too frequent in the early stages of operation and too far apart in the later stages (Chang et al., 2017).

2.3.3 Chemical cleaning

Even with periodic physical cleaning, irreversible fouling still accumulates in membrane systems since the desorption of adsorbed foulants such as proteins and macromolecules is a thermodynamically unfavourable process (Shi et al., 2014). To remove

this fraction of fouling, membranes are soaked in high-concentration chemical solutions for extended periods of time. This method is known as a clean-in-place when the membrane is left in the system but, to do so, adjustments must be made to the process equipment. The selection of chemical solution depends on the type of foulant to be removed and, often, the use of more than one cleaning solution is required. A list of chemical types, along with their functions, are presented in table 2.2.

Table 2.2: Common membrane cleaning agents and possible interactions with foulants (Shi et al., 2014)

Family	Examples	General functions
Acids	Strong: HCl, HNO_3 Weak: H_3PO_4, Citric	pH regulation, dissolution of inorganic precipitates, acidic hydrolysis of certain macromolecules
Alkalis	Strong: NaOH, KOH Weak: Na_2CO_3	ph regulation, alteration of surface charge, alkaline hydrolysis of proteins, catalysing saponification of fats
Oxidants	NaOCl, H_2O_2	Oxidation of organics, disinfection
Surfactants	Anionic: SDS Cationic: CTAB Nonionic: Tween 20	Dipersion/suspension of deposits
Chelants	EDTA	Complexation with metals, removal of mineral deposits
Enzymes	Proteases, lipases	Catalysing lysis of specific substrates (e.g., proteins, lipids)

In surface water applications, Alresheedi et al. (2019) showed that irreversible fouling caused by NOM on a ceramic ultrafiltration membrane was removed more substantially (>98%) when a sodium hydroxide clean-in-place (CIP) was followed by a sodium hypochlorite CIP or if the two solutions were mixed. The authors suggested that NaOH can loosen the adsorbed foulants by increasing their solubility and improving their contact with the NaOCl. In treatment applications involving

cyanobacteria, Zhang et al. (2011) demonstrated that sodium hypochlorite (100 mg/L, assumed to be expressed in terms of free chlorine) was best suited to clean a polyvinyl chloride ultrafiltration membrane fouled by *M. aeruginosa*. Indeed, compared to sodium hydroxide (500 mg/L), hydrochloric acid (500 mg/L), and EDTA (150 mg/L), it removed 88.4% of the irreversible fouling. By itself, sodium hydroxide (NaOH) was almost completely inefficient (1.5%) to remove irreversible cyanobacterial fouling. However, the authors demonstrated that NaOH altered the structure of the AOM. It can then be concluded that a CIP regime similar to the one proposed by Alresheedi et al. (2019) would be best to remove irreversible fouling caused by cyanobacteria.

2.3.4 Chemically-enhanced backwashes

A chemically-enhanced backwash (CEB) is a combination of both physical and chemical cleaning strategies. More specifically, a chemical is added to the backwash water to improve its performance and its main advantage is its short duration, compared to the duration of a CIP. Overall, the use of CEBs in drinking water treatment plants is relatively new. They appear to be promising as plants have reported decreasing the frequency of their CIP by a factor of four when initiating (Shi et al., 2014) but there appears to be very few detailed studies on their application. In a study by Fujioka and Nghiem (2015), ozone was dissolved in backwash solution and then flushed through a ceramic microfiltration membrane fouled by municipal wastewater. Once again, the results appeared to be promising: by backwashing the membrane for 3.5 minutes with 2 mgO3/L Milli-Q water, the membrane's specific flux was completely restored. Similar results were observed in seawater desalination CEB studies, mostly with chlorine (Chang et al., 2017). However, the data presented for the CEB in these studies were limited. A more detailed discussion on the research gap will be presented

in section 2.5.

2.4 Ozone for membrane fouling control

2.4.1 Chemistry of ozone-foulant interactions

Ozone is one of the most powerful oxidants (standard reduction potential of 2.07 V). Due to its electrophilic nature, it is highly reactive with unsaturated bonds. Therefore, humic substances and other natural organic matter components, which are composed of numerous aromatic rings, are highly reactive with ozone. In addition to direct reactions with organic matter, ozone naturally decomposes in water to form hydroxyl radicals. These radicals are short-lived but are known to be less selective and stronger oxidants (standard reduction potential of 2.80 V) than ozone (Van Geluwe et al., 2011). This indirect ozonation is considered one of many competing reactions that can take place during the ozonation of NOM. These competing reactions are best described by the Staehelin-Bühler-Hoigné model, which is illustrated in the work of Van Geluwe et al. (2011). For practical purposes, the rate of ozone decomposition increases, as pH and water temperature increase. The activation energy of the initiation reaction decreases as the hydroxide ion (OH-) concentration and as the water temperature increases (Nawrockia and Kasprzyk-Hordern, 2010).

Primarily, short-chain (less than 5 carbon atoms) carboxylic acids are the main products of ozone reactions with organic matter. These products are smaller and more hydrophilic and therefore, they are less likely to adsorb onto membrane surfaces. However, these compounds are not completely mineralized by ozone, even after large exposures. In contrast, hydroxyl radicals were shown to react rapidly with carboxylic acids. In fact, the first order reaction rate constants of radicals with these products

of ozonation are up to 10^{12} times greater than the rate constants observed for ozone alone. Although, it is worth noting that despite the reaction rate constants, a large portion of the main humic structure can remain intact during ozonation and radical oxidation. This is a result of steric hindrance, in which the large size of the humic substances prevents the oxidants from accessing and cleaving bonds anywhere but at the peripheries of the molecules (Van Geluwe et al., 2011).

The reaction rates of ozone with cyanobacteria varies between species due to varying cell size and nature of extracellular algal organic content. However, the reaction mechanisms are similar. Generally, ozonation of cyanobacteria suspensions increases the concentration of dissolved organic matter (DOC) in solution as a result of the direct transformation of cell membrane material into DOC and as a result of the release of intra-cellular DOC (Coral et al., 2013). Interestingly, there is agreement within the literature that ozone reactions with dissolved organic material precede cell lysis (Wei et al., 2016; Coral et al., 2013) and that cyanobacteria cell lysis is not required for cell death. In fact, the loss of cell membrane permeability in damaged cyanobacteria results in the oxidation of their nucleic material, effectively killing the cell. Furthermore, the loss of cell membrane integrity is rapid and was shown to occur at CT (concentration $*$ exposure time) values below 0.2 mg$*$min/L (measured with the integration of the ozone decay curve; 0.5 mgO_3/L initial ozone dose; total exposure of 0.5 minutes) via BacLight viability testing for both *M. Aeruginosa* and *Anabaena flos-aquae*. Complete cell lysis occurs later when exposed to high ozone doses (Coral et al., 2013).

2.4.2 Catalytic ozonation

Given the oxidative potential of hydroxyl radicals, the promotion of radical formation by solid metal oxides, such as the ones used to produce ceramic membranes, is of particular interest for membrane fouling control. In principle, dissolved ozone molecules adsorb on the membrane surface or in the pores and decomposes into hydroxyl radicals, which can react with other adsorbed organic foulants. For this adsorption, the metal cations of the ceramic oxide act as Lewis acid and base sites whereas the hydroxyl groups, which are present on the surface of the oxides, act as Brönsted acid sites (Nawrockia and Kasprzyk-Hordern, 2010). Since the quantity of hydroxyl groups present is dependent of the metal oxide, the difference between the water's pH and the oxide's piezoelectric point will determine the overall charge of the metal oxide, which in turn affects the oxide's adsorption capacity (Kasprzyk-Hordern et al., 2003).

The effects of such catalytic ozonation on the oxidation of NOM were analysed and differentiated from direct ozonation by Zhang et al. (2008). To do so, they exposed acid, neutral, and base fractions of both hydrophilic and hydrophobic NOM to ozone with and without powdered cerium oxide in solution. A larger DOC removal of all NOM fractions was obtained in the presence of the oxide (maximum DOC removal: 6.5% for ozonation alone and 47.8% for O_3/CeO_2). They also noted a slight improvement in UVA_{254} reduction. It is believed that this increase, or at least a portion of it, is caused by catalytic ozone activity given that the DOC removals in the ozonated solutions with cerium oxide were greater than the sum of individual DOC reductions by ozonation and by adsorption on cerium oxide alone.

2.4.3 Application of ozone with ceramic membranes

Of the membrane fouling control strategies discussed in section 2.3, the use of ozone in feed water alteration applications, in chemically-enhanced backwashes, and in clean-in-place procedures have been studied. The experimental conditions used in the studies that will be discussed below are summarized in table 2.3.

In feed pre-treatment applications, ozone in the gaseous state is continuously introduced either directly in the membrane tank/module (*in situ*) or at the bottom of a feed water tank (*ex situ*). In both cases, small bubbles are formed by diffusers to maximize contact with water, in a similar fashion to air sparging. Given the potential for catalytic ozonation by the ceramic membrane materials, *in situ* applications are more frequent in literature. Sartor et al. (2008) used this technique and halt the accumulation of irreversible fouling caused by surface water during 48-hour tests. After an initial drop in permeate flux, the hydraulic backwashes were sufficient to always recover approximately 80% of the membrane's specific flux, which is up to 4 times higher than without ozonation. The authors believe that the chemical properties and composition of the formed foulant cake layer are different when ozone is present in the membrane module. More precisely, the reactions between ozone, extra-polymeric substances, and with natural organic matter in the feed water results into the formation of a more porous cake layer on the membrane surface, of which the resistance is smaller than the cake formed without *in-situ* ozonation. However, the observed accumulation of organic matter at the bottom of the membrane tank, even with an ozone residual in the feed, indicates that ozone does not completely mineralize the organic particulates.

In a similar study, Zhang et al. (2013) noted that, in the initial phase of filtration (first 3 days), the trans-membrane pressure (TMP) increased at an identical rate

Table 2.3: Experimental conditions used in combined ozonation and ceramic membrane filtration studies

Reference	Fouling control method	Feed water composition	Operating conditions	Membrane characteristics	Ozonation parameters
Sartor et al. (2008)	*In-situ* pre-treatment	Surface water pH: 7.2 TOC: 12.1 mg/L Turbidity: 19 NTU	300 -mbar, constant pressure Duration: 48 h Backwash: 2 min at 900 -mbar every 150 min	Flat-sheet UF Pores: 80 nm	10-50 g/h in 3000 L tank 25 min contact time
Zhang et al. (2013)	*In-situ* pre-treatment	Surface water pH: 6.80 - 7.20 TOC: 3.3 - 4.3 mg/L DOC: 1.9 - 3.5 mg/L Turbidity: 14.0 - 23.0 NTU	Coagulation pre-treatment 100 LMH, constant flux Duration: 13 days Backwash: 3.5 min at 300 LMH every 4h	Flat-sheet UF Pores: 60 nm Material: Al_2O_3	2.0 - 2.5 mg/L 25 min contact time
Wei et al. (2016)	*In-situ* pre-treatment	0.6% NaCl solution 2.0×10^6 *M. aeruginosa* cells/mL DOC: 1.67 mg EOM/L	90 LMH, constant flux Duration: 35 min Backwash: end-of-experiment	Flat-sheet UF Pores: 60 nm	0, 0.5, 1, 2, and 5 mg/L
Alresheedi et al. (2019)	Clean-in-place	Deionized water pH: 7.5 DOC: 2.5 mg/L humic acids or sodium alginate Turbidity: 5 NTU Ca^{2+}: 0 or 75 mg $CaCO_3$/L	Dead-end 100 LMH, constant flux Duration: 24h Backwash: 20s at 2 bars every 4h	Tubular UF Pores: 0.01 μm Material: SiC	0.5 mg O_3/mg C in 4L DI water at 15 °C 1h recirculation at 0.1 m/s cross-flow velocity
Fujioka and Nghiem (2015)	Chemically-enhanced backwash	Municipal wastewater pH: 7.5 TOC: 63 mg/L Turbidity: 8.1 NTU	Dead-end 150 LMH, constant flux Backwash (or CEB): 300 LMH for 2.5 min	Tubular MF Pores: 0.2 μm Material: α-Al_2O_3	2 mg/L in 2L RO water at 20 °C CEB: 300 LMH for 2.5 min

whether or not the feed water was ozonated. After this initial phase, the TMP increased but more slowly with ozonation and, in the end, Zhang et al. (2013) were able to almost double membrane operation time between chemical clean-in-place operations. Additionally, it was found that membrane fouling was almost fully reversible at low TMP (18-22 kPa) but that fouling became almost completely irreversible at a TMP greater than 30 kPa. A key difference between this study and the study of Sartor et al. (2008) is the residual ozone concentration in the membrane permeate. In the study by Zhang et al. (2013), the residual is null and, presumably, ozone is not dosed in high enough quantities to alleviate fouling that accumulates within the membrane pore. Additionally, this means that ozone is not present in the backwash water like in Sartor et al. (2008), where permeate with an ozone residual is used for the backwash. Consequently, one disadvantage of *in-situ* ozonation is the need for large ozone concentrations, which can be costly in full-scale applications.

In-situ ozonation was also used to control membrane fouling in the treatment of surface waters contaminated with cyanobacteria. Wei et al. (2016) reported that greater ozone concentrations generally reduced the rate of membrane fouling, due in large part to the formation of a thinner and more porous cake layer, as observed by Sartor et al. (2008). A reduced resistance due to pore blocking was also noted, presumably due to residual ozone passing through the membrane and into the permeate. Interestingly, larger ozone doses did not always result in lower fouling. At 2 mg O_3/L, fouling accumulated more rapidly than when ozone was applied at doses of 1 mg O_3/L and 5 mg O_3/L. This is explained by the increase of feed DOC resulting from the lysis of cyanobacteria cells at larger ozone doses. The DOC can also foul the membrane and consequently, more ozone must be added to compensate for the additional foulants.

As expected, in the studies discussed, ozone reduced the size/molecular weight

of the organic foulants and increased their hydrophilicity. Consequently, in addition to the observed changes in fouling behaviour, changes in permeate quality were also reported. In fact, there was a noticeable increase in the membrane's permeate DOC concentration (Sartor et al., 2008; Zhang et al., 2013; Wei et al., 2016). To overcome this potentially negative impact on treatment, an activated carbon filter must either be installed post-membrane to adsorb a fraction of the organics (Sartor et al., 2008; Zhang et al., 2013) or the ozone dosage must be increased, as done by Wei et al. (2016), to effectively minimize the accumulation of cyanobacterial toxins in the permeate.

In contrast to the performance of *in-situ* ozonation, Alresheedi et al. (2019) showed that it was possible to clean a membrane with ozone in a one-hour CIP and obtain the same performance (>98% recovery) as a combined sodium hydroxide and sodium hypochlorite CIP. By monitoring the cumulative ozone demand and cumulative carbon mass removed from the membrane, Alresheedi et al. (2019) showed that the oxidation of hydrophilic NOM (alginate) was slower than the oxidation of hydrophobic NOM (humic acid). In fact, the hydrophilic NOM was removed slowly at first and only increased after 30 minutes of ozone exposure whereas the removal of hydrophobic NOM followed what resembled first-order kinetics.

2.5 Summary of research needs

Ozone has demonstrated potential to help reduce and control fouling by organic matter and cyanobacteria in ceramic ultrafiltration membrane applications. The use of chemically-enhanced backwashes to introduce ozone in the membrane module will likely decrease the ozone doses required for effective cleaning and will improve the contact between ozone and the membrane pores.

The number of publications addressing membrane fouling has been growing expo-

nentially since 1990 whereas the number publications addressing membrane cleaning has been growing linearly. In 2015, there were approximately five times more fouling papers (500) published than cleaning papers (100) (Chang et al., 2017). Presently, most existing studies are focused on seawater desalination, which generally address the application of low-pressure membranes as a pre-treatment step to reverse osmosis. Furthermore, the chemical used in these studies is limited mainly to chlorine (Chang et al., 2017) and, in some cases, hydrogen peroxide (Yu et al., 2019). There also appears to be opportunities for the optimization of CEB operational parameters. For instance, the frequency of the CEB and the oxidant dose varies greatly between studies (between every 1 to 24 hours; 1 to 500 mg/L Cl_2) with little clear rational on the values selected. Furthermore, few studies have examined chemicals other than chlorine and no studies found have evaluated the performance of a CEB to control membrane fouling in surface waters impacted by cyanobacterial blooms.

Chapter 3

Methodology

3.1 Cyanobacterial culture

Microcystis aeruginosa (CCPC 633, non-toxic strain) was purchased from the Canadian Phycological Culture Centre. This species was chosen as it is the prevalent cyanobacteria species in fresh surface water in Canada as well as globally (O'Neil et al., 2012). Additionally, this species has the smallest cell diameter and tends to grow as single cells in laboratory cultures. These are specifically problematic for treatment plants as they are the most likely to not be removed by conventional treatment processes such as coagulation and sedimentation (Campinas and Rosa, 2010).

The *M. aeruginosa* culture was incubated in modified (tripled sodium nitrate concentration) Bold's Basal Medium (BBM) growth media (recipe in appendix C), maintained at 21 ± 2 °C, with constant aeration, and under a 12 hours light/dark cycle (2000 lux, Phillips) to simulate normal growth conditions. A schematic representation of the culture setup is presented in figure 3.1.

The culture was split between two autoclaved 6 L borosilicate glass Erlenmeyer flasks, sealed with rubber stoppers. Air was pumped (Top Fin®40-gallon Aquarium

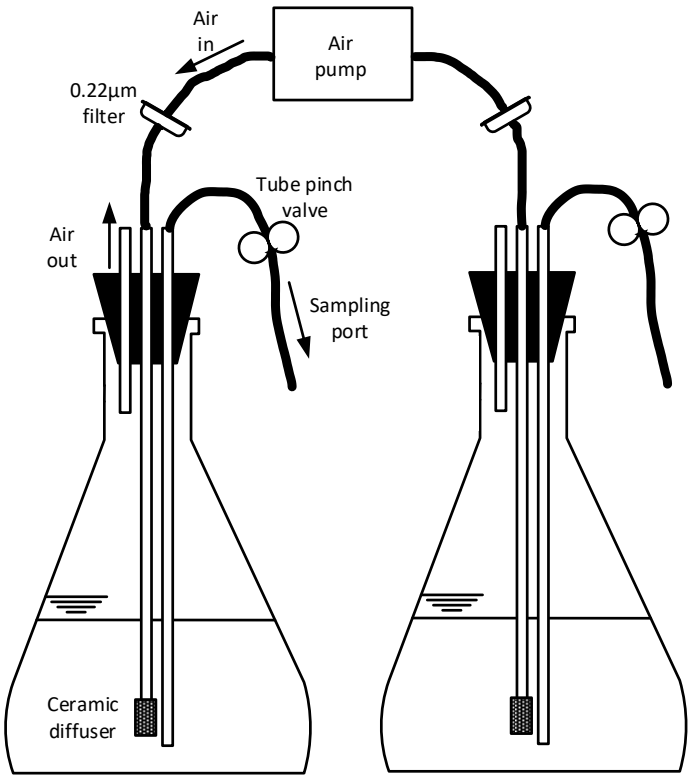

Figure 3.1: Schematic diagram of cyanobacteria culture setup

Air Pump) at the bottom of the flasks. To prevent culture contamination, the air was filtered through a polyethersulfone membrane with a pore size of 0.22 μm. Additionally, the flasks, stoppers, and all tubing were autoclaved before use. A venting tube was inserted through the stopper (but not into the culture) to prevent pressure build-up in the flask due to pumped air. A sampling tube was also inserted through the stopper. It was submerged in the culture, approximately 1 cm from the bottom of the flask, and pinched with a clamp at the exit. The flask was swirled manually prior to sampling to ensure the homogeneity of the culture. Also, a sterile syringe was used to collect the sample and the dead volume in the tubing was discarded before sampling.

The culture, which was split between the two flasks, were inoculated at different

times to maximize the availability of cyanobacteria for experiments and to act as backups for one another. The culture's growth was monitored by direct cell enumeration using an improved Neubauer hemocytometer (Marienfield) under 200x optical microscopy (Olympus BX 51). Each cell enumeration was duplicated, the average of which was used to calculate the cell concentration in the growth medium. On average, the single cells had a diameter of 4.11 $\pm$ 0.75 μm once in the stationary phase, that is, between 30 to 36 days after inoculation. The growth data is presented in figures 3.2 and 3.3.

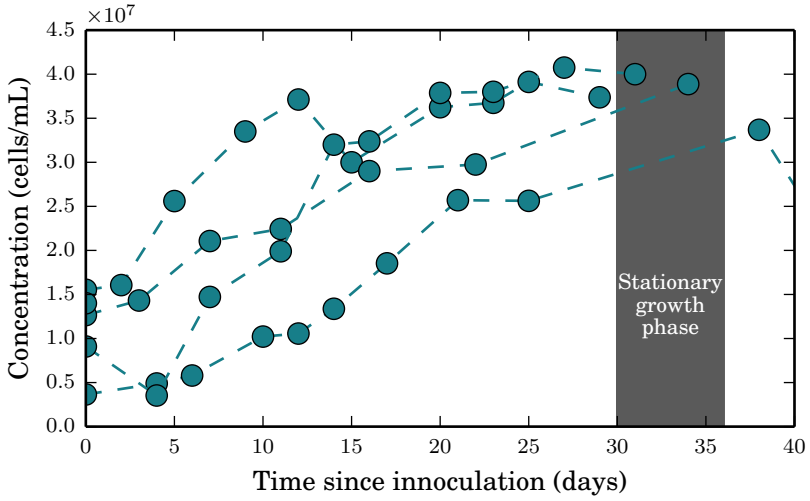

Figure 3.2: Growth of *Microcystis aeruginosa* (CPCC 633) in modified BBM medium.

Cell size measurements were taken by a Brightwell Dynamic Particle Analyser (model DPA-4100-INS-D, flow cell model 4002-003-001 SP1). The duplicate datasets were measured on different days, both within the 30 to 36 days after inoculation and with one culture re-inoculation between measurements. Cells were in surface water (discussed in section 3.2), which was diluted by a factor of 10 to respect the maximum allowable particle concentration of the instrument. The slight tail on the left of the distribution can be explained by dividing cells (effectively behaving as a pair) and

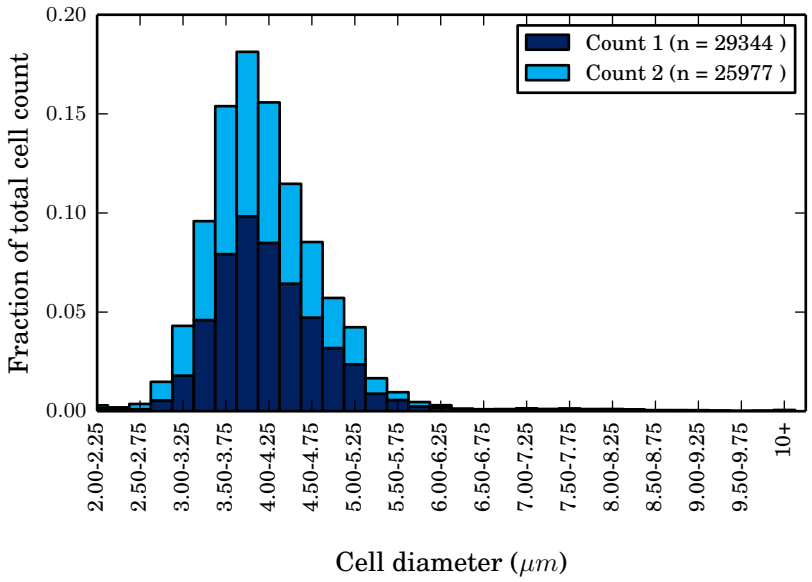

Figure 3.3: *Microcystis aeruginosa* (CPCC 633) cell size distribution in cyanobacteria-spiked surface water. The measurement was taken in duplicate (counts 1 and 2).

dead cells, which tend to agglomerate. All surface water particles should be smaller than 2 um since the sample was obtained post-filtration (as discussed in section 3.2).

3.2 Feed water

To fully understand the impact of different foulants present in surface water impacted by cyanobacteria on the performance of a chemically-enhanced backwash, three feed solutions were used in this study: surface water (SW), cyanobacteria-spiked ultrapure water (Cyano-UW), and cyanobacteria-spiked surface water (Cyano-SW).

The surface water (SW) was obtained from the Sainte-Rose Drinking Water Treatment Plant, the intake of which is located in the Rivière des Mille-Îles (Laval, Québec, Canada). The surface water used in the experiments was partially treated by the plant. It was collected from a sampling tap located at the outlet of sand-anthracite filters, which were downstream of alum coagulation, flocculation, and sedimentation

treatment steps. This surface water was collected weekly and was refrigerated (4°C). Prior to an experiment, the surface water was taken out of the refrigerator and left to warm up overnight in the laboratory.

To prepare the Cyano-UW feed solution, cyanobacteria cells were spiked into ultrapure water (Milli-Q™). The cyanobacteria cells were harvested in the stationary growth phase. They were first separated from the growth medium by centrifugation at 10 000 g and 4°C for 15 minutes (Qu et al., 2012a; Wei et al., 2016). The pellet was resuspended in an aliquot of the ultrapure water by vortexing for approximately 30 seconds and then transferred to the ultrapure water. The supernatant was filtered on a polyethersulfone filter (PALL Life Sciences) with a pore size of 0.45 μm to collect residual cells. These were also transferred to the ultrapure water. The centrifuged volume of culture was determined to obtain a cyanobacteria cell concentration of 5×10^5 cells/mL Cyano-UW feed. The same method was used to prepare the Cyano-SW feed solution, however the cyanobacteria cells were spiked into room-temperature surface water. It is worth noting that the pH of the ultrapure water (5.70) and surface water (6.90) are different but that it is suspected that it will have minimal impact on membrane fouling during filtration since they are between the piezoelectric points of the membrane materials (4 and 9 for zirconium dioxide and aluminum oxide respectively).

The total hardness of all three feed solutions was adjusted to 60 mg $CaCO_3$/L using calcium chloride dihydrate (Fisher Scientific) since divalent ions such as calcium and magnesium are known to impact membrane fouling. These ions were shown to reduce the foulants' negative surface charge, which weakens the electrostatic repulsive forces between foulants as well as between the foulants and the membrane surface (Qu et al., 2012b). The temperature of the feeds was maintained at room temperature (23 °C). The parameters of the three feed solutions are presented in chapter 4.

3.3 Bench-scale membrane filtration system

Experiments were conducted with a ceramic ultrafiltration membrane (Atech) installed on a semi-automated bench-scale filtration system. A schematic representation of the system is presented in figure 3.4. The membrane was tubular (inside-out flow), with a surface area of 95 cm^2 (length of 50 cm and internal diameter of 0.6 cm) and a molecular weight cut-off of 150 kDa. The membrane surface material was zirconium dioxide (ZrO_2), which was supported by a more porous layer of α-aluminum oxide (α-Al_2O_3).

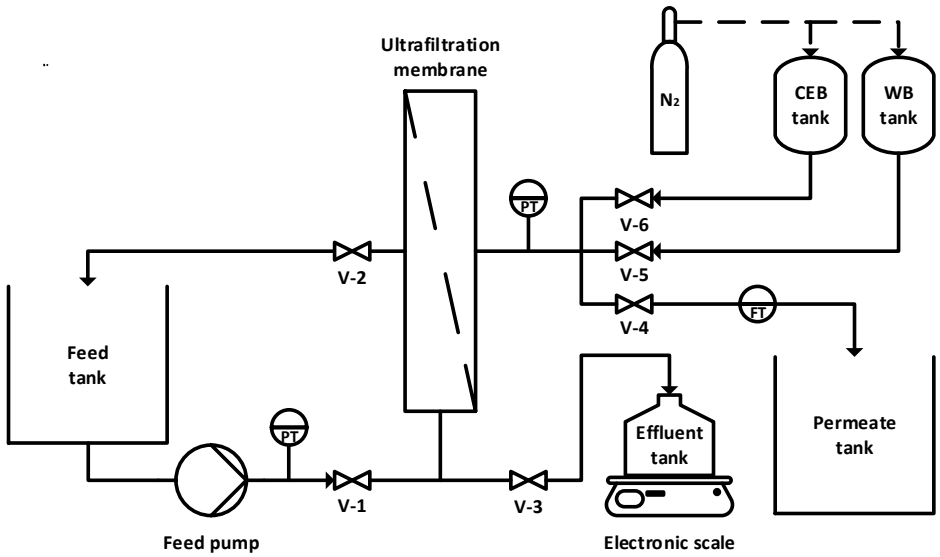

Figure 3.4: Schematic diagram of bench-scale ultrafiltration membrane system (PT: pressure transducer, FT: flow meter). Valves 1 and 4 are open during dead-end filtration; valves 3 and 5 are open during hydraulic backwashes; valves 3 and 6 are open during chemically-enhanced backwashes; and valves 1 and 2 are open during the end-of-experiment chemical washes.

The membrane was operated in dead-end filtration and was fed by a gear pump (drive: Ismatec BVP-Z; head: MicroPump L3468) to obtain a constant permeate flux of 200 liters per meter square of membrane surface per hour ($L/m^2/h$ or LMH). The permeate flowrate (flow sensor: McMillan Flow 101-3T) and trans-membrane pressure

(transducers: Omega PX309-100G5V) were measured every 30 seconds. Hydraulic (water-only) backwashes were initiated every 30 minutes and had a duration of 27 seconds (equivalent to 3 membrane volume replacements). Ultrapure water at room temperature and pressurized to 11.5 psig by nitrogen gas was used to obtain a flowrate of approximately 600 LMH during the hydraulic backwash.

Before each experiment, the permeability of the clean membrane was determined by filtering ultrapure water at 30 mL/min for 15 minutes and then repeating the procedure at flow rate increments of 10 mL/min, until a flow rate of 90 mL/min was reached.

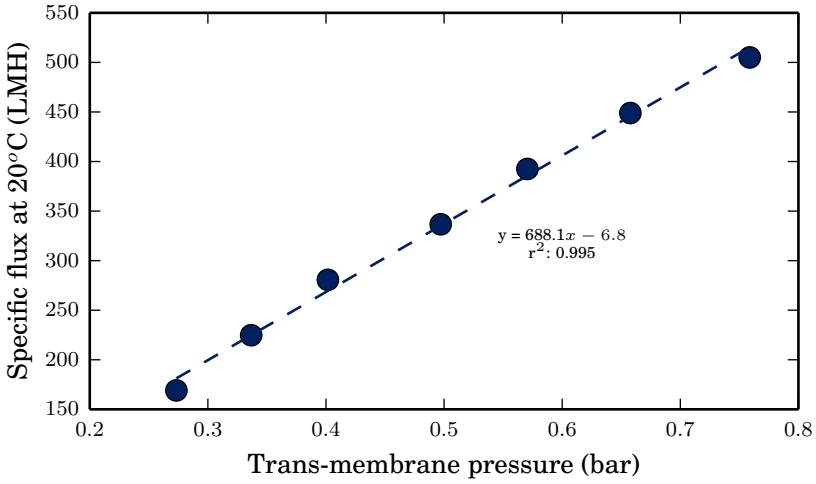

Figure 3.5: Determination of the clean membrane permeability by filtering ultrapure water (normalized to 20°C)

At the end of each experiment, the membrane was cleaned with a mixture of sodium hydroxide and sodium hypochlorite (pH 12, 500 mg/L as Cl_2, 35 °C) (Al-resheedi et al., 2019). To do so, the feed tank in figure 3.4 was replaced with the cleaning solution, which was recirculated at a cross-flow velocity of 0.1 m/s for 1 hour and then left to soak for 3 hours. This was followed by a hydrochloric acid wash to remove any residual organic and inorganic foulants. The HCl solution (pH 2) was

recirculated at 0.1 m/s for 1 hour, left to soak for 2 hours, and recirculated again for 1 hour (adapted from (Oligny et al., 2016)). Afterwards, the membrane system was flushed with ultrapure water until the pH of the permeate was stable.

3.4 Experimental plan

Three sets of experiments were conducted to address to the study's objectives: batch ozonation tests, baseline membrane performance tests, and ozone CEB tests.

3.4.1 Batch ozonation tests

The purpose of the batch ozonation tests is to determine and compare the reactivity of ozone with the different foulants in the feed solutions, without the interference of the CEB's hydraulic force or the membrane material, which reacts with ozone. To do so, a liter of each feed solution was placed in 2-liter borosilicate glass beakers, spiked with ozone, and continuously stirred. A small volume of highly concentrated ozone stock solution (50 - 60 mg/L) was added to obtain an ozone concentration of 2 milligrams per milligram of TOC in the feed solution. The stock was prepared by bubbling gaseous ozone, which was produced by a bench-top ozone generator (Ozone Solutions TG-10), in ultrapure water at 4°C to maximize ozone solubility. To minimize degassing, the aliquot of ozone stock solution was dosed with a syringe, feed solutions were covered with floating polytetrafluoroethylene lids, and water samples for analysis were taken with a syringe. Solutions were exposed to ozone for 30 minutes. Experiments were conducted at room temperature (23°C).

The ozone concentration of the stock solution and the ozone residual in solution throughout the tests were determined by using the indigo colorimetric method (Bader and Hoigné, 1981). More specifically, 0.5%, 1% and 3% indigo trisulfonate solutions

were prepared and a 20 mL sample of each were placed in individual 45 mL glass vials. To measure the ozone concentration in the stock solution, 0.3 mL of stock was added with a syringe to the 3% sample and 0.3 mL of ultrapure water was added to another 3% sample. The difference in absorbance at 600 nm (quartz cuvette, 1-cm pathlength) was used to calculate the ozone concentration in the stock solution (see sample calculations in appendix B). The ozone concentrations in the batch solutions during the tests were measured similarly. However, 4 mL of solution or ultrapure water was added to the indigo sample instead of 0.3 mL. Also, the solution or ultrapure water was added to a 1% indigo sample. If the indigo color of the sample was lost completely (clear), the ozone concentration was measured in with the 3% indigo sample. If the change in color in the 1% indigo sample was insignificant, the ozone concentration was measured in with the 0.5% indigo sample.

3.4.2 Baseline membrane performance tests

The purpose of the baseline tests is to determine the membrane fouling mechanisms involved when filtering the feed solutions and to evaluate their impact on fouling control by hydraulic backwashes. To do so, the feed solutions where filtered on the bench-scale membrane system discussed in section 3.3. Extended hydraulic backwashes (equivalent to a 2 mgO_3/mgC CEB) were initiated every 2 hours, of which the performance will be compared to the performance of CEBs in the ozone CEB tests.

3.4.3 Ozone CEB tests

Two series of CEB experiments were conducted. Firstly, ozone chemically-enhanced backwashes with a duration of 30 minutes were initiated after 2 hours of filtration on

the bench-scale membrane system described in section 3.3, during which the residual ozone concentration in the effluent and the cumulative organic matter removed from the membrane were monitored. This experiment was repeated with each feed solution and a control, which was a 30-minute CEB of the clean membrane. The purpose of the 30-minute CEB is to determine the foulant removal kinetics by ozone and to compare them to the kinetics observed during the batch ozonation tests.

Secondly, the purpose of the second set of ozone CEB experiments is to evaluate the impact of the ozone dose on the post-CEB membrane resistance. To do so, the Cyano-SW feed was filtered for 6 hours on the bench-scale membrane system described in section 3.3, during which an ozone CEB was initiated every 2 hours. The experiment was repeated with different CEB ozone doses, which was was varied by adjusting the CEB duration. To normalize the results, the dose were expressed as a function of the organic carbon mass remaining on the membrane surface prior to the CEB, as determined by mass balances.

In both sets of experiments, each CEB was preceded by a hydraulic backwash to specifically evaluate the impact of ozone on the hydraulically irreversible fouling fraction. The ozonated water used in the CEBs was prepared by diffusing gaseous ozone directly into the CEB reservoir filled with ultrapure water at 4 °C, similarly to the method presented in section 3.4.1. Once the ozone concentration was 40 mg/L, the reservoir was pressurized to 11.5 psig and the CEB was started immediately. The dissolved ozone concentration in the stock CEB solution and in the CEB effluent was determined with the indigo method, as described in section 3.4.1, except that only the residual ozone in the CEB effluent was measured in duplicate (0.3 mL in 20 mL of 3% indigo solution). To minimize ozone degassing when sampling, the extremity of the CEB effluent line was submerged in an overflowing 45 mL vial. Samples could then be taken from the center of the vial with a syringe.

To summarize, the operating conditions used during the membrane filtration tests (baseline membrane performance tests and ozone CEB tests) are listed in table 3.1.

Table 3.1: Summary of membrane filtration experiments

Parameter	Units	Baseline	30-minute CEB	Varied O_3 dose
Filtration flux	LMH	200	200	200
Hydraulic backwash frequency	hours	0.5	0.5	0.5
Backwash flux	LMH	600	600	600
Backwash duration	seconds	27	27	27
CEB frequency	hours	2	2	2
CEB flux	LMH	600	600	600
CEB O_3 concentration	mg/L	0	40	40
Filtered feed solutions	-	SW Cyano-UW Cyano-SW	SW Cyano-UW Cyano-SW	Cyano-SW

3.5 Analytical methods

In addition to specific monitored parameters discussed above, the pH (Hach 2100), the total and dissolved organic carbon concentrations (Sievers M5310C On-Line TOC Analyzer), the ultraviolet absorbance at 254 nm (Cary UV-vis, Varian) were measured. Fluorescence excitation-emission matrices (FEEM) were also obtained (Shimadzu 5301PC). Excitation and emission wavelengths were set to range between 220 and 600 nm, with an excitation increment of 10 nm, an excitation slit width of 10 nm, an emission slit width of 5 nm, and a sampling interval of 1.0 nm. In the batch tests, these measurements were taken for the feed before and after ozonation. In the baseline and CEB experiments, the measurements were taken for the feed, permeate, hydraulic backwash (cumulative for all hydraulic backwash between two CEBs), and CEB effluents.

Chapter 4

Ozone chemically-enhanced backwash for the control of ceramic membrane fouling by cyanobacteria

Stéphane Venne[a], Onita D. Basu[a], Benoit Barbeau[b]

[a]Department of Civil and Environmental Engineering, Carleton University, 1125 Colonel By Drive, Ottawa, ON, Canada K1S 5B6

[b]Department of Civil, Geological and Mining Engineering, Polytechnique, C.P. 6079 Succursale Centre-Ville, Montréal, QC, Canada, H3C 3A7

Keywords: Ceramic ultrafiltration, Cyanobacteria fouling, Ozone, Chemical cleaning, Chemically-enhanced backwash

4.1 Introduction

The increasing frequency and intensity of harmful cyanobacteria (algae) blooms in surface freshwater, due primarily to eutrophication and climate change (O'Neil et al., 2012), poses challenges to drinking water treatment plants. The rapid changes in cell

densities and their tendency to float can result in inefficient treatment by coagulation and result in cell breakthrough to settled water (Coral et al., 2013). Meanwhile, low-pressure ultrafiltration (UF) membranes can completely remove cyanobacteria cells, even the smallest ones (*Microcystis aeruginosa*, 3-6 μm), from water by size exclusion (Campinas and Rosa, 2010) and with minimal cell breakage (Qu et al., 2012a). However, membrane productivity rapidly decreases due to fouling by cyanobacteria cells and natural organic matter (NOM) present in surface water. Cyanobacteria cells form a compressible cake layer on the membrane (Qu et al., 2012a; Liu et al., 2017) whereas NOM adsorbs on the membrane surface as well as within the membrane pores (Hofs et al., 2011; Xia et al., 2013). Consequently, fouling increases operation costs and remains, especially the hydraulically irreversible fouling fraction (i.e. fouling not removed by hydraulic backwashes), the greatest obstacle to the application of membranes in drinking water treatment. (Gao et al., 2011; Shi et al., 2014).

To remove hydraulically irreversible fouling, a chemical cleaning is most commonly executed as a clean-in-place (CIP) operation, which requires that the membrane be soaked in chemicals for extended periods of time (Shi et al., 2014). The drawbacks of a CIP are that it requires process adjustments, requires large chemical concentrations, and results in costly downtime (Shi et al., 2014). A chemically-enhanced backwash (CEB) is an alternative strategy in which a chemical, at a relatively small concentration compared to a CIP, is combined with a hydraulic backwash for an *in-situ* cleaning process that results in downtimes similar to those of hydraulic backwashes (Chang et al., 2017).

In drinking water treatment, chlorine is the mostly used chemical in CIP and CEB procedures. However, the application of this oxidant in a CEB results in the formation of undesirable trihalomethanes and halogens in water with high organic content, such as surface water dominated by cyanobacteria blooms. There are also

concerns that frequent chlorine applications will cause the formation of carbonate scale in the membrane module, a type of fouling that must be removed by an acid CIP at low pH (≤ 2) (Chang et al., 2017).

A potential alternative to chlorine is ozone. Ozone is of particular interest for CEB applications as it reacts more rapidly than chlorine with organic material in water (Van Geluwe et al., 2011) and smaller exposures (as small as 0.2 mg·min/L) are required to damage cyanobacterial cells (Coral et al., 2013). Furthermore, the catalytic decomposition of ozone by ceramic materials leads to the formation of stronger and less selective oxidants, making the combination of ozone and ceramic membranes very attractive, yielding new opportunities for membrane fouling control (Van Geluwe et al., 2011). In comparison, polymeric membranes, which are presently more widely used in water treatment plants due to their lower capital cost (Chang et al., 2017), are actually damaged by repeated exposure with oxidants (Gao et al., 2011).

When ozone was used in a clean-in-place (CIP) procedure to clean a ceramic ultrafiltration membrane fouled by humic acids and alginate fractions of NOM, over 98% of the unified membrane fouling index (UMFI) was recovered within an hour. In that application, a dissolved ozone solution was recirculated with a normalized dose of 0.5 mg O_3 per mg of organic carbon on the membrane at the start of the CIP. The performance of the ozone CIP is comparable to a 4-hour CIP with a mixed solution of sodium hydroxide and hypochlorite (Alresheedi et al., 2019).

Sartor et al. (Sartor et al., 2008) used continuous *in-situ* ozonation, a technique in which ozone is continuously dosed in the membrane module during filtration, to control ceramic membrane fouling by surface water. In this study, the rate of fouling was reduced and hydraulic backwashes maintained the membrane's specific flux at approximately 80% of its original value, which is up to 4 times higher than without *in-situ* ozonation. In the presence of the cyanobacterium *M. aeruginosa* (2×10^6

cells/mL, DOC: 1.67 mg/L), Wei et al. (Wei et al., 2016), also reported that *in-situ* ozonation (0-5 mg/L) reduced the rate of UF membrane fouling. The authors of both studies hypothesized that the reactions between ozone, the extrapolymeric substances, and the natural organic matter in the feed water lead to the formation of a more porous cake layer on the membrane surface. This more porous cake resulted in a membrane foulant resistance that was smaller than foulant resistance caused by the cake formed without *in-situ* ozonation.

The application of *in-situ* ozonation reduces the rate of membrane fouling but this type of application is energy-intensive and requires the continuous addition of ozone to be effective (Schlichter et al., 2004). A greater ozone demand is expected as ozone can react with all the feed components, not only what fouls the membrane. Furthermore, in treatment applications involving cyanobacteria, ozone can induce the release of the cells' internal organic metabolites (Coral et al., 2013). These metabolites can be toxic (O'Neil et al., 2012), increase the fraction of fouling that is hydraulically irreversible (Wei et al., 2016), and permeate through the membrane (Wei et al., 2016). In these cases, there is an increase in the permeate's dissolved organic carbon concentration and an adsorptive media such as granular activated carbon is required downstream to remove these components and ensure regulatory compliance (Sartor et al., 2008).

The chemically-enhanced backwash (CEB) does not suffer from the disadvantages of CIPs and continuous *in-situ* ozonation. However, research addressing the mechanisms and kinetics involved in CEB fouling control applications is limited. The impact of an ozone CEB on membrane fouling was quantified, in which ozone could almost completely remove the fouling caused by filtration of municipal wastewater on a ceramic microfiltration membrane over several filtration cycles (Fujioka and Nghiem, 2015). The authors suggested that this performance was due to increased ozone reactions with foulants within the membrane pores. Most of the other studies

regarding CEB applications applied a chlorine CEB for membrane fouling control in seawater desalination and feed water that has a low particulate organic matter concentration. The CEB was rarely the primary focus of these studies, which generally address the application of low-pressure membranes as a pretreatment step to reverse osmosis. Additionally, the frequency of the CEB and the oxidant dose varied greatly between studies (between every 1 to 24 hours; 1 to 500 mg/L Cl_2), and the chosen doses where not justified (Chang et al., 2017). Studies analyzing the impact of CEB parameters on performance have not been found for surface water applications nor cyanobacteria-laden water applications.

The objective of this research is to demonstrate the potential of ozone chemically-enhanced backwashes to control the fouling of ceramic ultrafiltration membranes by cyanobacteria in surface water and to understand the cleaning mechanisms involved in the process. This will be achieved by: (1) comparing the performance of an ozone CEB to the performance of a hydraulic (water-only) backwash, (2) determining the rate of ozone demand and organic foulant removal from the membrane during an ozone CEB, and (3) evaluating the effect of ozone dose on foulant removal and membrane resistance. From a general perspective, this research will help determine the importance of different CEB parameters, which is information required to optimize the impact of a chemically-enhanced backwash on membrane fouling control.

4.2 Materials and methods

4.2.1 Cyanobacterial culture

Microcystis aeruginosa (CCPC 633, non-toxic strain) was purchased from the Canadian Phycological Culture Centre (Waterloo, Ontario, Canada). It was incubated in

3N-BBM growth media, at 21 ± 2 °C, with constant aeration, and under a 12 hours light/dark cycle to simulate normal growth conditions (2000 lux, Phillips). *M. aeruginosa* was chosen for this study as it is the predominant freshwater cyanobacterial species (O'Neil et al., 2012) and has the smallest single cell diameter. Small single cells are problematic as they are the most likely to not be removed by coagulation and sedimentation (Campinas and Rosa, 2010). The culture's growth was monitored by direct cell enumeration using an improved Neubauer hemocytometer (Marienfield). On average, the single cells had a diameter of 4.11 ± 0.75 μm once in the early stationary phase, between 30 to 36 days after inoculation.

4.2.2 Feed water

To fully understand the impact of different foulants present in surface water impacted by cyanobacteria on the performance of a chemically-enhanced backwash, three feed solutions were used in this study: surface water (SW), cyanobacteria-spiked ultrapure water (Cyano-UW), and cyanobacteria-spiked surface water (Cyano-SW).

The surface water was obtained from the Sainte-Rose Drinking Water Treatment Plant, of which the intake is located in the Rivière des Mille-Îles (Laval, Québec, Canada). The surface water used in the experiments was collected after alum coagulation and flocculation, sedimentation, and sand-anthracite filtration. To prepare the Cyano-UW feed solution, cyanobacteria cells were spiked into ultrapure water (Milli-Q™) and to prepare the Cyano-SW feed, cyanobacteria were spiked into the surface water. The cells were harvested in the early stationary growth phase and were separated from the growth medium by centrifugation at 10 000 g and 4°C for 15 minutes (Qu et al., 2012a; Wei et al., 2016). The final cyanobacteria cell concentration in both the Cyano-UW and Cyano-SW feeds was 5×10^5 cells/mL.

The parameters of the three feed solutions are listed in table 4.1. Since divalent ions were shown to impact membrane fouling (Qu et al., 2012b), the total hardness of all three feed solutions was adjusted to 60 mg $CaCO_3$/L using calcium chloride dihydrate (Fisher Scientific). During the experiments, the temperature of the feeds was maintained at room temperature (23 ± 1 °C).

Table 4.1: Average feed water parameters

Parameter	Units	SW	Cyano-UW	Cyano-SW
pH	-	6.90 ± 0.221	5.70 ± 0.078	7.18 ± 0.326
Turbidity	NTU	0.133 ± 0.0218	1.92 ± 0.141	2.23 ± 0.371
TOC	mg/L	2.81 ± 0.197	1.97 ± 0.318	4.58 ± 0.231
DOC	mg/L	2.81 ± 0.197	0.127 ± 0.0311	2.76 ± 0.283
UV_{254}	cm^{-1}	0.053 ± 0.003	0.035 ± 0.003	0.088 ± 0.001
SUVA	$L/mg * m$	1.90 ± 0.069	1.77 ± 0.117	1.93 ± 0.069

4.2.3 Bench-scale membrane filtration system

Experiments were conducted with a ceramic ultrafiltration membrane (Atech) installed on a semi-automated bench-scale filtration system. A schematic representation of the system is presented in figure 4.1. The membrane was tubular, with a surface area of 95 cm^2 and a molecular weight cut-off of 150 kDa. The membrane surface was composed of zirconium dioxide (ZrO_2) and supported by an α-aluminum oxide (α-Al_2O_3) layer.

The membrane was operated in dead-end and was fed by a gear pump (drive: Ismatec BVP-Z; head: MicroPump L3468) to obtain a constant permeate flux of 200 LMH. Given the high mechanical strength of ceramic membranes, the permeate flux was set higher than average to accelerate fouling. The permeate flowrate (flow sensor: McMillan Flow 101-3T) and trans-membrane pressure (transducers: Omega PX309-

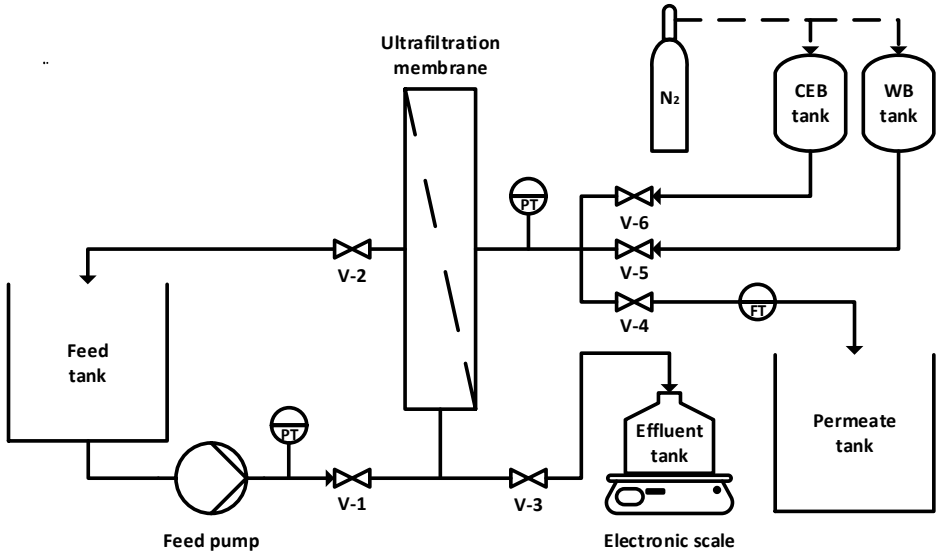

Figure 4.1: Schematic diagram of bench-scale ultrafiltration membrane system (PT: pressure transducer, FT: flow meter). Valves 1 and 4 are open during dead-end filtration; valves 3 and 5 are open during hydraulic backwashes; valves 3 and 6 are open during chemically-enhanced backwashes; and valves 1 and 2 are open during the end-of-experiment chemical washes.

100G5V) were measured every 30 seconds. Hydraulic (water-only) backwashes were initiated every 30 minutes and had a duration of 27 seconds (equivalent to 3 membrane volume replacements). Ultrapure water at room temperature and pressurized to 11.5 psig by nitrogen gas was used to obtain a flowrate of approximately 600 LMH during the hydraulic backwash.

At the end of each experiment, the membrane was washed with a mixed solution of sodium hydroxide and sodium hypochlorite (pH 12, 500 mg/L as Cl_2, 35 °C) (Alresheedi et al., 2019). To do so, the feed tank in figure 4.1 was replaced with the cleaning solution, which was recirculated at a cross-flow velocity of 0.1 m/s for 1 hour and then left to soak for 3 hours. This was followed by a hydrochloric acid wash to remove any residual organic and inorganic foulants. The HCl solution (pH 2) was recirculated at 0.1 m/s for 1 hour, left to soak for 2 hours, and recirculated again for

1 hour (adapted from (Oligny et al., 2016)). Afterwards, the membrane system was flushed with ultrapure water until the pH of the permeate was stable.

4.2.4 Experimental plan

Three sets of experiments were conducted to address the research objectives: batch ozonation tests, baseline membrane performance tests, and ozone CEB tests.

Batch ozonation tests

The purpose of the batch ozonation tests is to determine and compare the reactivity of ozone with the different foulants in the feed solutions, without the interference of the CEB's hydraulic force or the membrane material, which reacts with ozone. To do so, a liter of each feed solution was placed in 2-liter borosillicate glass beakers, spiked with ozone, and continuously stirred. A small volume of highly concentrated ozone stock solution (50 - 60 mg/L) was added to obtain an ozone concentration of 2 milligrams per milligram of TOC in the feed solution. The stock was prepared by bubbling gaseous ozone, which was produced by a bench-top ozone generator (Ozone Solutions TG-10), in ultrapure water at 4°C. To minimize degassing, the aliquot of ozone stock solution was dosed with a syringe, feed solutions were covered with floating polytetrafluoroethylene lids, and water samples for analysis were taken with a syringe. Solutions were exposed to ozone for 30 minutes. Experiments were conducted at room temperature (23°C). The ozone concentration in solution throughout the tests was determined by using the indigo colorimetric method, described elsewhere (Bader and Hoigné, 1981).

Baseline membrane performance tests

The purpose of the baseline tests is to determine the membrane fouling mechanisms involved when filtering the feed solutions and to evaluate their impact on fouling control by hydraulic backwashes. To do so, the feed solutions where filtered on the bench-scale membrane system discussed in section 4.2.3. Extended hydraulic backwashes (solution with 0 mgO_3/L with the same duration as a 2 mgO_3/mgC CEB) were initiated every 2 hours, of which the performance will be compared to the performance of CEBs in the ozone CEB tests.

Ozone CEB tests

Two series of CEB experiments were conducted. Firstly, 30-minute long ozone chemically-enhanced backwashes were initiated after 2 hours of filtration on the bench-scale membrane system described in section 4.2.3, during which the residual ozone concentration in the effluent and the cumulative organic matter removed from the membrane were monitored. This experiment was repeated with each feed solution. A control experiment, which is a 30-minute CEB of the clean membrane, was also conducted to estimate the ozone demand from the ceramic membrane itself given its reactivity with ozone. Overall, the purpose of the 30-minute CEB is to determine the foulant removal kinetics by ozone and to compare them to the kinetics observed during the batch ozonation tests.

Secondly, the purpose of the second set of ozone CEB experiments is to evaluate the impact of the ozone dose on the post-CEB membrane resistance. To do so, the Cyano-SW feed was filtered for 6 hours on the bench-scale membrane system described in section 4.2.3, during which an ozone CEB was initiated every 2 hours. The experiment was repeated with different CEB ozone doses, which were varied by

adjusting the CEB duration. To normalize the results, the doses were expressed as a function of the organic carbon mass remaining on the membrane surface prior to the CEB, as determined by mass balances.

In both sets of experiments, each CEB was preceded by a hydraulic backwash to specifically evaluate the impact of ozone on the hydraulically irreversible fouling fraction. The ozonated water used in the CEBs was prepared by diffusing gaseous ozone directly into the CEB reservoir filled with ultrapure water at 4 °C, similarly to the method presented in section 4.2.4. Once the ozone concentration was 40 mg/L, the reservoir was pressurized to 11.5 psig and the CEB was started immediately. The dissolved ozone concentration in the stock CEB solution and in the CEB effluent was determined with the indigo method. To minimize ozone degassing when sampling, the extremity of the CEB effluent line was submerged in an overflowing 45 mL vial. Samples could then be taken from the center of the vial with a syringe.

4.2.5 Analytical methods

In addition to specific monitored parameters discussed above, the pH, the turbidity (Hach 2100), the total and dissolved organic carbon concentrations (Sievers M5310C On-Line TOC Analyzer), the ultraviolet absorbance at 254 nm (Cary UV-vis, Varian) were measured. Fluorescence excitation-emission matrices (FEEM) were also obtained (Shimadzu 5301PC). Excitation and emission wavelengths were set to range between 220 and 600 nm, with an excitation increment of 10 nm, an excitation slit width of 10 nm, an emission slit width of 5 nm, and a sampling interval of 1.0 nm. In the batch tests, these measurements were taken for the feed before and after ozonation. In the baseline and CEB experiments, the measurements were taken for the feed, permeate, hydraulic backwash (cumulative for all hydraulic backwash between

two CEBs), and CEB effluents.

4.3 Results and discussion

4.3.1 Ozone kinetics in batch tests

In the batch test experiments, each feed was spiked with two milligrams of ozone per milligram of TOC in solution and continuously stirred. As illustrated in figure 4.2, ozone reacts more rapidly with the components in surface water (SW) than with cyanobacteria cells (Cyano-UW).

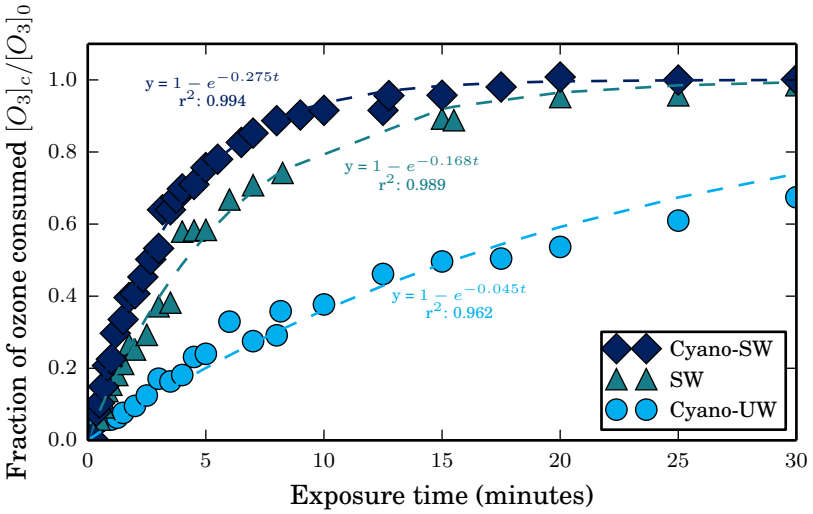

Figure 4.2: Cumulative ozone demand (normalized) in 1L batch solutions: surface water (SW), cyanobacteria-spiked ultrapure water (Cyano-UW) and cyanobacteria-spiked surface water (Cyano-SW). Ozone spiked to obtain a concentration of 2 mg of ozone per mg of total organic carbon (TOC) in solution. Experiments conducted at 23°C.

Reaction rate constants, which are independent of reactant concentrations, can be used to quantify the ozone kinetics in the different feed solutions and confirm the above observation. To do so, the constants are obtained by rearranging the general reaction rate law in equation 4.1.

$$-\frac{d[O_3]}{dt} = k[O_3][TOC] \tag{4.1}$$

Where $[O_3]$ is the ozone concentration in solution, t is the exposure time, k is the reaction rate constant, and [TOC] is the total organic carbon concentration in solution. For simplicity, it is assumed that the rate is first order with respect to reactant concentrations. Also, it is assumed that the TOC concentration in solution remains constant throughout the batch experiments. Although the TOC concentrations measured before and after ozonation are indeed almost identical (data not shown), considering the TOC concentration as constant in equation 4.1 remains an assumption since the structure and chemical properties of the various organic molecules that the TOC measurement quantifies changes when they are oxidized. Therefore, their reactivity with ozone also changes (Van Geluwe et al., 2011). The increases in DOC to TOC ratios (SW: 0.00% since all DOC initially, Cyano-UW: 69.9%, Cyano-SW: 31.4%) and the decreases in UV_{254} absorbances (SW: 69.2%, Cyano-UW: 46.2%, Cyano-SW: 57.9%) after ozonation supports this statement.

With the assumptions listed above, the expression $[O_3] = [O_3]_0 - [O_3]_c$, where $[O_3]_0$ is the initial dissolved ozone concentration and $[O_3]_c$ is the cumulative ozone consumed, can be substituted in equation 4.1. Integrating the resulting equation with respect to time yields equation 4.2, which can be used to fit the data in figure 4.2. As written, the rate of reaction appears to be of pseudo-first order.

$$\frac{[O_3]_c}{[O_3]_0} = 1 - e^{-[TOC]\cdot k\cdot t} \tag{4.2}$$

The rate constants are extracted from the fits by dividing the exponent by the initial TOC concentration (in moles). The resulting rate constants are 7.43×10^2, 2.46×10^2, and 6.79×10^2 mol^{-1} L min^{-1} for the SW, Cyano-UW, and Cyano-SW

solutions, respectively. The SW rate constant is greater than the Cyano-UW rate constant and confirms that ozone reacts more rapidly with the surface water components than with cyanobacteria.

4.3.2 Baseline membrane fouling and hydraulic reversibility

Ultrafiltration reduced the turbidity, DOC, and UV_{254} of the SW solution by 40.7%, 6.8%, and 11.6%, respectively. In contrast, the feed turbidity, TOC, DOC, and UV_{254} were reduced by 95.5%, 99.0%, 84.3% and 100.0% during the filtration of Cyano-UW and were reduced by 96.5%, 42.6%, 4.9% and 47.0% during the filtration of Cyano-SW. Since the membrane is operated in dead-end filtration, the solution components removed by the membrane are therefore, the membrane foulants. The resulting progressive decreases in membrane specific flux are illustrated in figure 4.3.

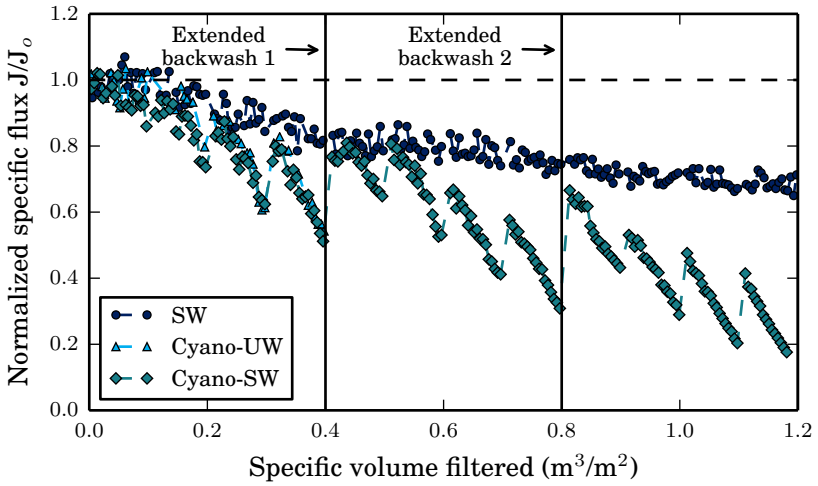

Figure 4.3: Decrease in the membrane's specific flux during constant flux, dead-end filtration (200 LMH) of different feed solutions. The horizontal dashed line indicates the clean membrane flux. The Cyano-UW data only extends to 0.4 m^3/m^2 and is almost fully superimposed by the Cyano-SW data.

The decrease in specific flux caused by the SW and Cyano-UW solutions indicate that both surface water components and cyanobacteria cells foul the membrane.

However, since the specific flux decrease caused by the Cyano-SW is almost identical to the decrease caused by Cyano-UW feed solution, it can be concluded that the cyanobacteria cells have a greater impact on total fouling than surface water components.

As seen in the fluorescence excitation-emission matrices of the feed and membrane permeate solutions presented in figure 4.4, the surface water organic matter appears to be mainly composed of humic and fulvic substances (peaks A and C), as well as a small fraction of polysaccharides (peak T). The FEEM of the SW membrane permeate is similar to the FEEM of the SW feed solution, which indicates that the majority of the organic matter in SW is not intercepted by the membrane. This is also reflected by the small DOC removal of 6.8%. It is likely that the majority of NOM molecules are smaller than the membrane pores given that the water was collected post-sand/anthracite filtration at the drinking water treatment plant. Consequently, it is expected that the removed surface water NOM is adsorbed on the membrane surface and within its pores. This is supported by the decreasing specific membrane flux for SW in figure 4.3, which appears to reach a steady-state, as it would in an adsorption isotherm.

In comparison, the presence of cyanobacteria cells in ultrapure water (Cyano-UW) is identified by two peaks in the proteinic regions of the FEEM (T peaks). In this case, the FEEM of the Cyano-UW permeate indicate that the cells are completely removed by the membrane, as also suggested by the 99.0% TOC removal. Given that the cyanobacteria cells are much larger than the membrane pores, they form a cake layer on the membrane surface. Interestingly, the intensity of the A and C FEEM peaks in the permeate are reduced when filtering the Cyano-SW. It is likely that the cyanobacteria cake acts as a filter aid.

Moreover, the cake formed by cyanobacteria is shown to be compressible by fitting

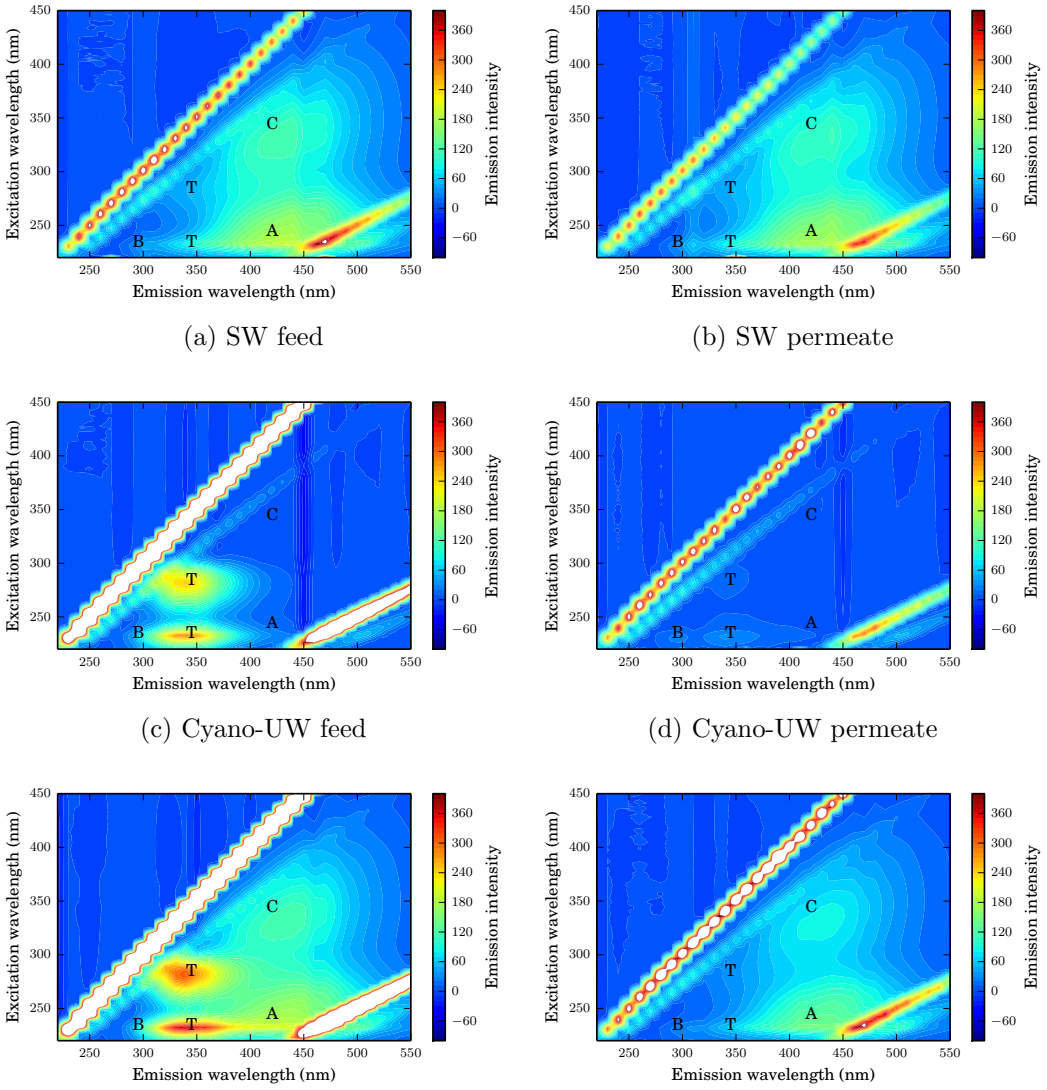

(a) SW feed

(b) SW permeate

(c) Cyano-UW feed

(d) Cyano-UW permeate

(e) Cyano-SW feed

(f) Cyano-SW permeate

Figure 4.4: Fluorescence excitation-emission matrices of membrane feed and permeate streams. The peaks A (excitation/emission: 237-260/400-500 nm) and C (excitation/emission: 300-370/400-500 nm) represent the humic-like and fulvic-like substances. The B (excitation/emission: 225-237/309-321 and 275/310 nm) and T (excitation/emission: 225-237/340-381 and 275/340 nm) peaks represent the tyrosine protein-like and the tryptophan protein-like substances. The peak A also represents hydrophobic acids, whereas the peak B represents the hydrophobic neutrals and the T peaks represent the hydrophobic bases, the hydrophilic acids, and the hydrophilic neutrals (Hudson et al., 2007).

the trans-membrane pressures (ΔP) measured in the Cyano-SW baseline experiment to the model developed by Chellam and Xu (Chellam and Xu, 2006) for microbial suspensions (equation 4.3).

$$\Delta P = \Delta P_0 + \frac{Q\mu\alpha_0(1+n\Delta P)c_b}{A_0}V_s \tag{4.3}$$

Where ΔP_0 is the trans-membrane pressure at the beginning of a filtration cycle, Q is the flow rate, A_0 is the membrane surface area, μ is the water viscosity, α_0 is the specific cake resistance at no pressure, c_b is the bulk concentration, V_s is the specific volume filtered, and n is the cake compressibility factor. The fitted data is presented in figure 4.5.

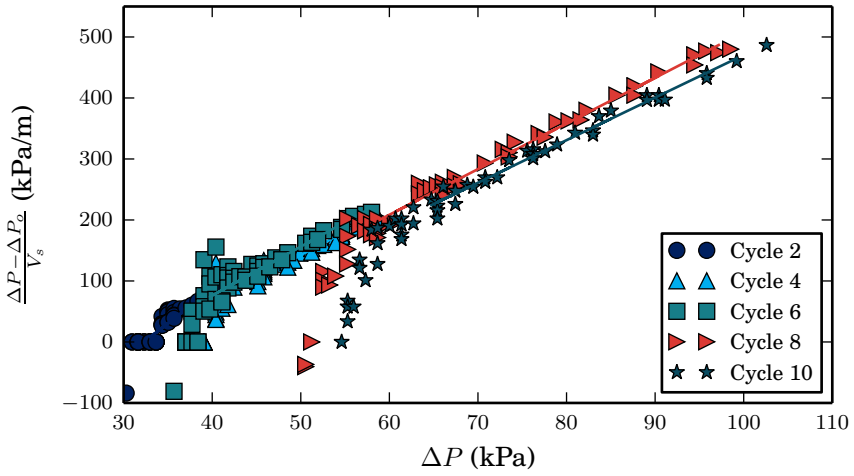

Figure 4.5: Compressibility of foulant cake layer formed on the membrane surface during the filtration of Cyano-SW. A cycle is defined as the filtration period between two hydraulic backwashes.

The average compressibility factor of the cake layer is 3.15 ± 0.08 × 10^{-2} m^2/N, which is relatively large (a value of 0 represents an incompressible cake) (Chellam and Xu, 2006). Only the linear portion of the plots were fitted, all with $R^2 > 0.90$. Similar compressibility factors were obtained when fitting the Cyano-UW data (3.02

$\pm$ 0.11×10^{-2}). It is believed that the non-linear portion of data is the result of under-developed cake formation, where other types of fouling mechanisms might be taking place.

In figure 4.3, the decrease in specific flux caused by this fouling is not reversed by hydraulic backwashes when the membrane is fouled by SW. In fact, given the absence of peaks in the FEEM of the SW hydraulic backwash effluent, as seen in figure 4.6, suggests that the hydraulic backwash is completely ineffective. This supports the idea that natural organic matter adsorbs on the membrane surface and within the membrane pores since desorption is a thermodynamically unfavourable process and, therefore, is not removed by hydraulic forces (Shi et al., 2014).

In comparison, the hydraulic backwashes help recover the membrane's specific flux when the membrane is fouled by cyanobacteria (Cyano-UW and Cyano-SW). This is confirmed by the FEEM of the Cyano-UW and Cyano-SW hydraulic backwash effluents, in which intense proteinic (T) peaks are observed and suggests that this recovery is mainly due to the removal of cyanobacteria cells from the membrane surface.

However, although the hydraulic backwashes considerably improve the membrane specific flux for the Cyano-UW and Cyano-SW feeds, a fraction of the fouling remains irreversible as seen by incomplete recovery. In fact, after 0.4 m^3 of filtered solution per m^2 of membrane (immediately before the extended backwash), there was 0.67, 1.54, and 2.16 milligrams of SW, Cyano-UW, and Cyano-SW TOC (respectively) remaining on the membrane surface and within its pores.

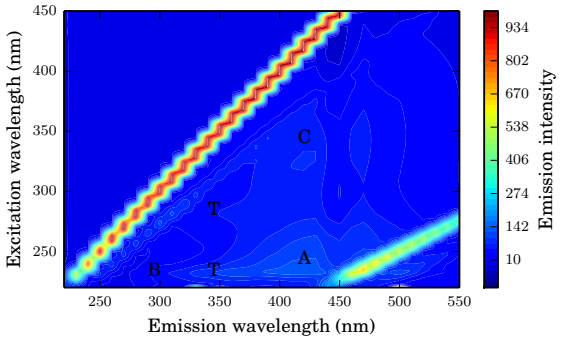

(a) SW

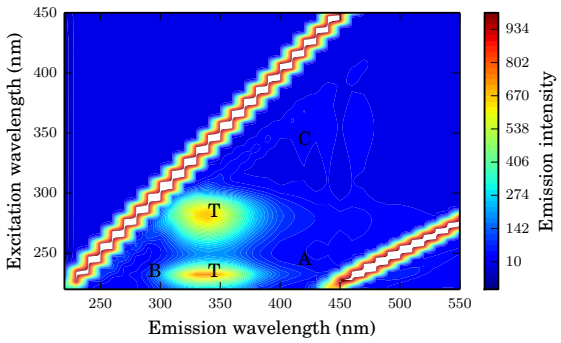

(b) Cyano-UW

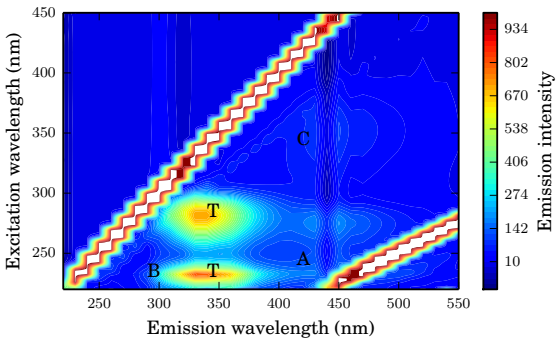

(c) Cyano-SW

Figure 4.6: Fluorescence excitation-emission matrices of hydraulic backwash effluents. The peaks A (excitation/emission: 237-260/400-500 nm) and C (excitation/emission: 300-370/400-500 nm) represent the humic-like and fulvic-like substances. The B (excitation/emission: 225-237/309-321 and 275/310 nm) and T (excitation/emission: 225-237/340-381 and 275/340 nm) peaks represent the tyrosine protein-like and the tryptophan protein-like substances. The peak A also represents hydrophobic acids, whereas the peak B represents the hydrophobic neutrals and the T peaks represent the hydrophobic bases, the hydrophilic acids, and the hydrophilic neutrals (Hudson et al., 2007).

4.3.3 Ozone chemically-enhanced backwash kinetics

To control hydraulically irreversible fouling, a 30-minute ozone chemically-enhanced backwash was executed after 0.4 m^3/m^2 specific volume of feed solution filtered. The residual ozone concentration and the cumulative TOC in the effluent were monitored throughout the CEB, the results of which are presented in figure 4.7.

The initial rate of removal of Cyano-UW foulants (cyanobacteria cells) is similar to the removal of SW foulants in the first 5 minutes of the CEB. The initial rate of Cyano-SW foulants is also similar, suggesting that this initial removal is independent of the selectivity of ozone, as opposed to what was observed in the batch tests. This is comfirmed by quantifying the ozone reaction kinetics with the reaction rate constants, similarly to the batch tests. The constants are obtained by rearranging the general reaction rate law in equation 4.4.

$$-\frac{d[TOC]}{dt} = k[O_3][TOC] \tag{4.4}$$

Where [TOC] is the total organic carbon concentration on the membrane, t is the CEB duration, and $[O_3]$ is the dissolved ozone concentration in the membrane module. Again, for simplicity, it is assumed that the rate is first order with respect to concentrations. It is also assumed that the dissolved ozone concentration in the membrane module, $[O_3]$, is constant throughout the CEB. This is a valid assumption given that fresh ozone stock solution is continuously introduced in the membrane module during the CEB and that the residence time of water inside the module is only 8.9 seconds. A pseudo-first order rate equation can be obtained by substituting $[TOC] = [TOC]_0 - [TOC]_e$, where $[TOC]_0$ is the TOC on the membrane at the start of the CEB and $[TOC]_e$ is the cumulative TOC collected in the CEB effluent, in equation 4.4 and integrating it with respect to time. The resulting equation, equation

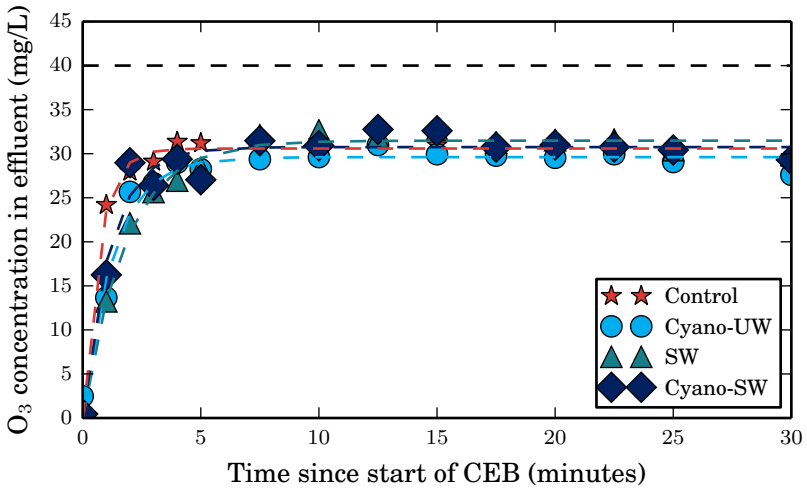

(a)

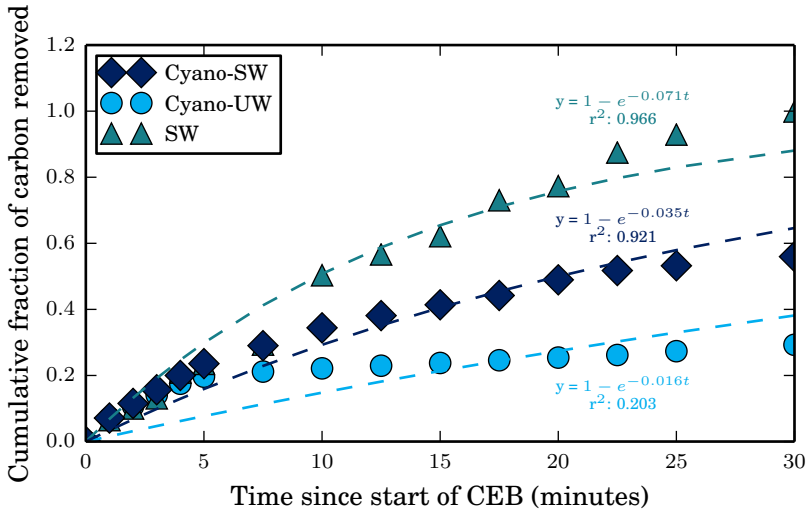

(b)

Figure 4.7: a) Residual ozone concentration and b) accumulated TOC in effluent at different times throughout a 30-minute ozone CEB. The dissolved ozone concentration in the CEB influent was maintained at 40 mg/L, as indicated by the dashed horizontal line in figure a). The CEB flux was approximately 600 LMH.

4.5, can be used to fit the data in figure 4.7b.

$$\frac{[TOC]_e}{[TOC]_0} = 1 - e^{-[O_3]\cdot k\cdot t} \tag{4.5}$$

The rate constants are extracted from the fits by dividing the exponent by the initial ozone concentration (in moles). The resulting rate constants are 8.51×10^1, 1.92×10^1, and 4.16×10^1 in mol^{-1} L min^{-1} for the SW, Cyano-UW, and Cyano-SW solutions, respectively. The first-order fit of the SW foulant removal is relatively good (R^2: 0.966). However, the first-order fit does not correlate well with the removal of Cyano-UW foulants (R^2: 0.203). Arguably, the first 5 minutes of the Cyano-UW CEB (and of the Cyano-SW) would be best represented by zero-order kinetics. This suggests that the removal of irreversible fouling caused by cyanobacteria is not simply due to its reactivity with ozone but due to the combination of ozone and the CEB's hydraulic force. More precisely, ozone likely alters the foulants' surface chemistry and, in turn, weakens the cake's structure and increases its porosity. Therefore, it is more easily removed by hydraulic forces. The importance of the hydraulic shear might be less important in the case of SW NOM given that it is likely adsorbed in the membrane pores, as discussed in section 4.3.2.

Altogether, the observations discussed above highlight the potential important impacts of CEB parameters on its performance. For instance, a greater CEB flux could possibly increase foulant removal and, furthermore, complete cyanobacteria disintegration by ozone might not be required for foulant removal from the membranes. In other words, ozone doses may not need to be as large as 19 mgO_3/mgC (equivalent ozone dose for a 30 minute CEB when the membrane is fouled by Cyano-SW) as a smaller dose might sufficiently weaken the cake structure for it to be removed by the CEB's hydraulic force. The previous statement is especially true given that, after

the first 7 minutes of the CEB, the unreacted residual ozone concentrations in the CEB effluents are relatively large, as seen in figure 4.7a. Additionally, the residual ozone concentrations after the first 7 minutes of the CEB are the same in the SW, Cyano-UW, and Cyano-SW experiments, as well as in the control experiment (CEB on a clean membrane). Therefore, the net ozone demand (defined as the residual ozone concentration in the effluent of the SW, Cyano-UW, or Cyano-SW subtracted from the residual ozone concentration in the control's CEB effluent), is effectively null at this point. Consequently, no additional TOC is removed in the Cyano-UW CEB. Interestingly, carbon is still removed from the membrane in the SW and Cyano-SW CEBs. Given that there is a 10 mg/L difference between the CEB influent and effluent in all experiments, including the control, it is believed that ozone reacts with the membrane material. Whether ozone is adsorbed on the membrane or decomposed into highly reactive hydroxyl radicals through catalytic ozonation Kasprzyk-Hordern et al. (2003), it could explain the continued foulant removal. More precisely, the adsorbed ozone and the radicals might be reacting with the SW NOM adsorbed in the membrane pores.

4.3.4 Effect of ozone dose on CEB performance

The impact of the 30-minute CEB discussed in section 4.3.3 on the membrane's specific flux is illustrated in figure 4.8.

When the membrane was fouled by SW, its specific flux was fully recovered after the CEB and was even maintained during filtration afterwards. As mentioned in section 4.3.3, this is likely due to the reactivity of ozone in the ceramic membrane pores, which mitigates the diffusion of SW NOM (Zhang et al., 2013). Full recovery was actually expected since the 30-minute CEB completely removed the organic matter

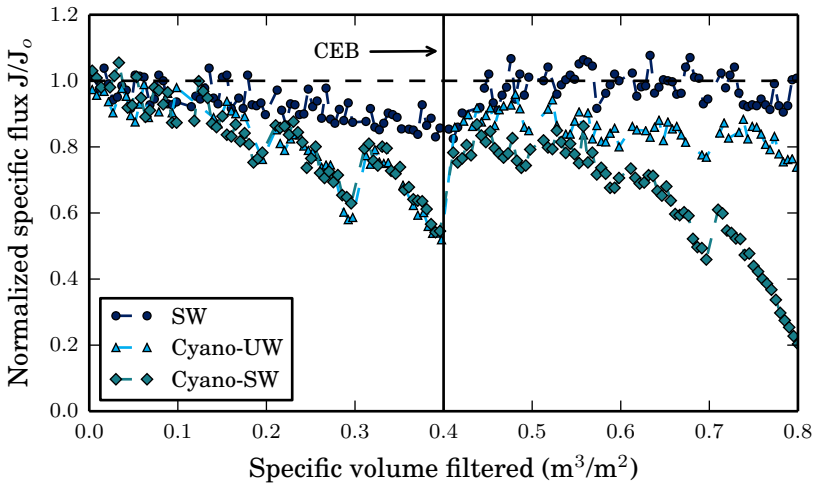

Figure 4.8: Decrease in the membrane's specific flux during constant flux, dead-end filtration (200 LMH) of different feed solutions. The horizontal dashed line indicates the clean membrane flux. A 30-minute ozone CEB was initiated after 2 hours of filtration (600 LMH, 40 mgO_3/L).

that was left on the membrane before the CEB, as seen in figure 4.7b. In contrast, no organic matter is removed after 7 minutes of the Cyano-UW CEB, yet there is still 1.14 mg of TOC (74%) on the membrane according mass balances. It is suspected that leftover cell debris adsorbed on the membrane surface and in the pores could explain why only approximately 80% of the specific flux is recovered by the CEB when the membrane is fouled by Cyano-UW and Cyano-SW solutions. In fact, it was previously shown that cyanobacteria cells are not fully disintegrated by ozone (Coral et al., 2013). This was also observed in the batch ozonation tests, in which there was a residual of 0.8 mgO_3/mgC in the Cyano-UW solution after a 30-minute exposure and in which the ozone consumption rate became almost null (see figure 4.2). Yet, the increase in the DOC/TOC fraction from 6.4% to 46.2% indicates that particulate organic matter (cells and associated debris) were still in solution. If the cell debris is adsorbed into the membrane pores, it is probably difficultly removed by the CEB's hydraulic shear force.

Nonetheless, more SW NOM is removed with CEB duration in the Cyano-SW experiment. However, the 30-minute CEB is equivalent to an ozone dose of 19 mgO_3/mgC in the Cyano-SW experiment, which is relatively large. To assess the impact of the ozone dose on the CEB performance, the experiments were repeated with different CEB durations to obtain ozone doses of 1, 2, and 4 mgO_3/mgC. Two subsequent CEB cycles were also run, as illustrated in figure 4.9.

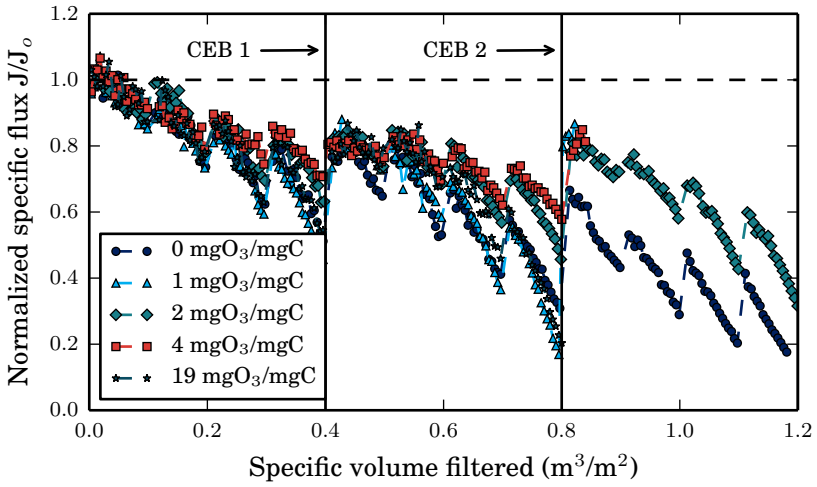

Figure 4.9: Impact of ozone CEB dosage on the membrane's specific flux decrease during constant flux, dead-end filtration (200 LMH) of cyanobacteria-spiked surface water (Cyano-SW). The horizontal dashed line indicates the clean membrane flux.

To quantify the resistance caused by fouling throughout the experiments illustrated in figure 4.9, Darcy's law was used (Wei et al., 2016), as written in equation 4.6.

$$R = \frac{\Delta P}{\mu * J} \tag{4.6}$$

Where R is the total resistance, ΔP is the trans-membrane pressure, μ is the water viscosity, and J is the flux of water through the membrane. The intrinsic membrane resistance was calculated from the flux and pressure recorded while filtering ultrapure

water through the clean membrane. On average, it was $5.63 \pm 0.27 \times 10^{11}$ m^{-1}. The resistance caused by the remaining foulants after a hydraulic backwash (or a CEB) was determined by calculating the total resistance immediately after the hydraulic backwash (or the CEB) and subtracting the average intrinsic membrane resistance. It can be assumed that the error in fouling resistances is in the same order of magnitude as the average intrinsic membrane resistance. The resistance caused by irreversible Cyano-SW foulants are presented in figure 4.10. On average, for all ozone doses tested, the resistances before CEB 1 and CEB 2 were $1.03 \pm 0.13 \times 10^{12}$ $m^{-1}$and 1.91 $\pm$ 0.93×10^{12} m^{-1}. The relatively large standard deviations for these resistances is a result of the variability of the cyanobacteria culture's state over the study's duration and due to the achievable accuracy of cell counts when preparing the volumes of feed required for the experiments. It is worth noting that the unified membrane fouling index (UMFI) was not used to analyze fouling since the UMFI cake filtration model was developed for incompressible cakes (Huang et al., 2008), which was shown in section 4.3.2 to not be the case when filtering cyanobacteria-laden water.

As in the 30-minute CEB, the membrane resistance is greater than the clean membrane resistance after an ozone chemically-enhanced backwash for all tested ozone doses. After CEB 1, the remaining fouling resistances are similar in all experiments, including the baseline (0 mgO_3/mgC) experiment. In other words, the addition of ozone in CEB 1 was only marginally advantageous. After CEB 2, the resistance is 45.8% smaller than in the 0 mgO_3/mgC experiment when the ozone dose is greater than 0. It is likely that the cake layer was more compressed under the larger transmembrane pressure required to maintain a constant permeate flux before CEB 2. Ozone can weaken the structural integrity of this compressed cake layer and increase its porosity by reacting with cells and the dissolved organic matter adsorbed onto them (Wei et al., 2016). Additionally, the zeta potential of damaged cells is more

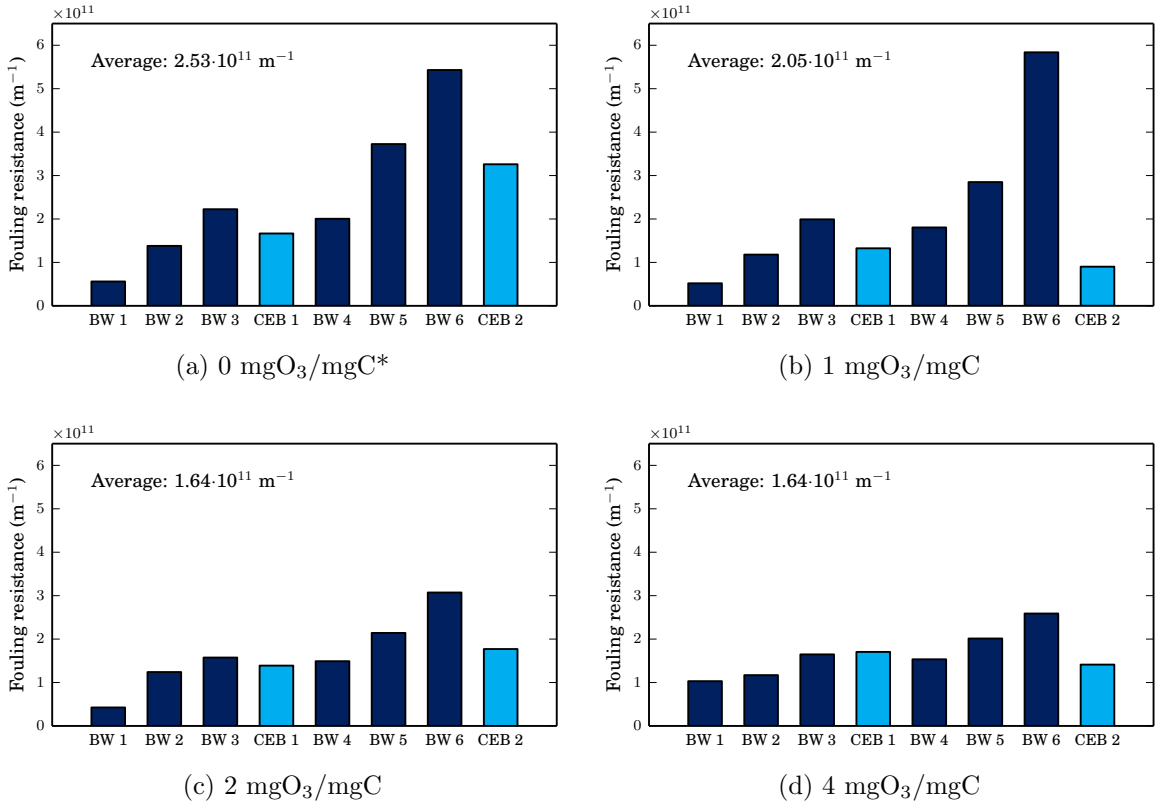

(a) 0 mgO_3/mgC*

(b) 1 mgO_3/mgC

(c) 2 mgO_3/mgC

(d) 4 mgO_3/mgC

Figure 4.10: Membrane fouling resistances after hydraulic backwashes (BW) and ozone chemically-enhanced backwashes (CEB) initiated during the filtration of Cyano-SW. The average fouling resistance of all cycles is provided as a metric to capture the effect of repeated CEB on long-term membrane performance. *In the baseline experiment (0 mgO_3/mgC), the CEB was replaced with an extended hydraulic backwash.

negative than the zeta potential of live cells (Liu et al., 2017), strengthening the repulsive electrostatic forces between themselves, organic foulants, and the membrane. Presumably, the CEB's hydraulic force can more easily remove the weakened foulant cake layer. Once again, the importance of the CEB's hydraulic force is highlighted. It can even be concluded that when membrane fouling is dominated by a compressible cake, the role of ozone is to transform the hydraulically irreversible fouling into hydraulically reversible fouling. Given that from a practical perspective it would complex to manage the waste generated by an ozone CEB, it might be simpler to optimize the hydraulic backwash parameters (frequency - not necessarily on a time basis, duration, flux) to control membrane fouling caused by cyanobacteria.

An observation of interest is that the resistance after CEB 2 is only slightly higher on average than the resistance after CEB 1 in experiments where the ozone dose is greater than 0 mgO_3/mgC. It is possible that ozone chemically-enhanced backwashes can keep the fouling resistance fairly constant. In other words, CEB-irreversible fouling accumulates at a very slow rate between CEBs. For economic purposes, it would be interesting to determine the smallest ozone dose required to maintain this performance.

The ozone dose, when greater than 0, does not result in considerable differences in membrane resistance immediately after CEB 1 and CEB 2. This conclusion is contradictory to what would be expected from the results of the 30-minute CEB, in which more organic matter was removed with increasing CEB duration (Cyano-SW), as seen in figure 4.9. More precisely, it was expected that a greater organic matter removal would result in a decrease of foulant resistance but that was not the case. As mentioned earlier, the removal of TOC after 7 minutes of CEB is due to NOM removal, which is believed to adsorb in the membrane pores and have less of an impact on fouling resistance than cyanobacteria cells. Interestingly however, larger

ozone doses appear to reduce the rate of irreversible fouling between CEBs, likely due to greater removal of NOM from within the membrane pores. This is captured by the average fouling resistance over all 8 cycles presented in figure 4.10, which initially decreases rapidly but appears to stabilize at doses above 2 mgO_3/mgC.

4.4 Conclusions

In summary, over two filtratio cycles, periodic ozone chemically-enhanced backwashes with doses between 1 and 19 mgO_3/mgC were capable of restoring up to 80% of the ceramic ultrafiltration membrane's specific flux when fouled by cyanobacteria-laden surface water. It was also possible to completely restore the specific flux when the membrane was fouled by surface water only. The following insights on the mechanisms involved in ozone chemically-enhanced backwashes were gained:

1. In batch test ozonation, the components in surface water react more rapidly with ozone than with cyanobacteria. However, the reverse is observed during a CEB, suggesting that complete foulant degradation by ozone is not required to remove the foulants. Instead, ozone likely weakens the structure of the cake layer, which increases its porosity and can be more easily removed by the CEB's hydraulic force. This is an improvement over the hydraulic backwash in the second filtration cycle where a large trans-membrane pressure is sustained, resulting in a more highly compressed foulant cake.

2. The ozone CEB can maintain the membrane's specific flux at 80% of its original value. Ozone doses between 1 and 19 mgO_3/mgC does not impact this recovery and therefore, a relatively small ozone dose could be used to maintain CEB performance. However, the rate of fouling accumulation between CEBs is

reduced when larger ozone doses are applied, likely due to greater removal of NOM from within the membrane pores during the CEB.

Acknowledgements

The authors of this paper would like to thank Carleton University and the Canadian National Science and Engineering Research Council for funding this research. They would also like to thank Marie Tudoret, Jacinthe Mailly, Julie Philibert, Yves Fontaine, Gabriel St-Jean, Mireille Blais, and Tetiana Elyart for their help installing the membrane system, troubleshooting methods, and their assistance during data collection. Finally, they would like to thank the members of the Basu research group as well as the members of the CREDEAU research team for their continued support and feedback.

Chapter 5

Conclusions

5.1 Summary

In this research, a ceramic membrane fouled by surface water components and cyanobacteria cells was intermittently exposed to ozone during chemically-enhanced backwashes. Over two filtration cycles (one cycle represents a specific filtered volume of 0.4 m^3/m^2 of membrane), it was possible to recover at least 80% of the membrane's specific flux with an ozone CEB. After the first filtration cycle, this represents little improvement over a traditional hydraulic backwash but after the second filtration cycle, it actually represents a 48.5% improvement in membrane flux recovery. Based on this difference, it is suspected that ozone weakens the structure of the compressible cake layer formed by cyanobacteria on the membrane surface, which would be more tightly compressed by the large trans-membrane pressures sustained at the end of the second filtration cycle. In other words, when the membrane is fouled by cyanobacteria cells, the role of ozone is to transform the hydraulically irreversible fouling into hydraulically reversible fouling, which is then removed by the CEB's hydraulic shear force. The importance of the hydraulic component is confirmed when comparing the

reaction kinetics of ozone with foulants in batch tests and during a CEB. In the batch test, ozone reacts more rapidly with surface water components than with cyanobacteria cells. This selectivity is not observed in during the CEB. Initially, surface water foulants and cyanobacteria cells are removed at a similar rate. Once the foulant interactions are weakened by ozone oxdiation, the hydraulic force of the CEB can remove these foulants from the membrane. Therefore, complete mineralization by ozone is not necessary for efficient membrane cleaning and a small ozone dose could result in similar CEB performance. In fact, of the four ozone CEB doses tested (1, 2, 4, and 19 mg O_3/mg C), the specific flux recoveries after two CEB cycles were almost identical for all doses. Interestingly, ozone appeared to reduce the rate of membrane fouling between CEBs, contrarily to what was hypothesized. It is concluded that this is due to greater removals of surface water contaminants from within the membrane pores. Furthermore, contrarily to what was hypothesized, the ozone demand is not a good predictor of foulant removal due to its catalytic decomposition on the membrane material, which produces highly reactive radicals that can also oxidize foulants.

5.2 Potential future CEB research

It would be interesting to explore the long-term impact of ozone chemically-enhanced backwashes on membrane fouling control and to determine if the membrane's specific flux can be maintained at approximately 80% of its original value over several subsequent CEBs. There are also several opportunities for optimization within the CEB process itself. For instance, to reduce ozone costs and residual concentrations in the effluent (which is wasted and needs to be treated before discharge), it would be useful to determine the minimum ozone dose required to maintain the observed performance. Additionally, the performance of the CEB could potentially be improved

by varying the hydraulic parameters, such as the CEB flux.

From a more general membrane fouling control perspective, it would be beneficial to confirm that catalytic ozonation actually has an impact on the removal of irreversible fouling (whether it be with cyanobacteria fouling or other types of organic fouling). More precisely, a deeper understanding of the mechanisms, kinetics, and effects of radical formation during a CEB (and any other combination of ozonation and ceramic membrane filtration) would allow research to optimize the application of catalytic ozonation and maximize its potential for fouling control.

References

Alresheedi, M. T., Basu, O. D., and Barbeau, B. (2019). Chemical cleaning of ceramic ultrafiltration membranes - ozone versus conventional cleaning chemicals. *Chemosphere*, 226:668–677.

Amin, S. K., Abdallah, H. A. M., Roushdy, M. H., and El-Sherbiny, S. A. (2016). An overview of production and development of ceramic membranes. *International Journal of Applied Engineering Research*, 11:7708–7721.

Babel, S. and Takizawa, S. (2011). Microfiltration membrane fouling and cake behavior during algal filtration. *Desalination*, 261:46–51.

Bader, H. and Hoigné, J. (1981). Determination of ozone in water by the indigo method. *Water Research*, 15:449–456.

C. Ho, J. and Michalak, A. M. (2015). Challenges in tracking harmful algal blooms: A synthesis of evidence from lake erie. *Journal of Great Lakes Research*, 41:317–325.

Campinas, M. and Rosa, M. J. (2010). Evaluation of cyanobacterial cells removal and lysis by ultrafiltration. *Separation and Purification Technology*, 70:345–353.

Chang, H., Liang, H., Qu, F., Liu, B., Yu, H., Du, X., Li, G., and Snyder, S. A. (2017). Hydraulic backwashing for low-pressure membranes in drinking water treatment: A review. *Journal of Membrane Science*, 540:362–380.

Chellam, S. and Xu, W. (2006). Blocking laws analysis of dead-end constant flux microfiltration of compressible cakes. *Journal of Colloid and Interface Science*, 301:248–257.

Coral, L. A., Zamyadi, A., Barbeau, B., Bassetti, F. J., Lapollib, F. R., and Prevost, M. (2013). Oxidation of microcystis aeruginosa and anabaena flos-aquae by ozone: Impacts on cell integrity and chlorination by-product formation. *Water Research*, 47:2983–2994.

De Souza, N. P. and Basu, O. D. (2013). Comparative analysis of physical cleaning operations for fouling control of hollow fiber membranes in drinking water treatment. *Journal of Membrane Science*, 436:28–35.

ESA (2019). Algal blooms in lake erie (north america). https://earth.esa.int/web/earth-watching/environmental-hazards/content/-/article/algal-blooms-in-lake-erie-north-america. Accessed: 2019-11-02.

Fujioka, T. and Nghiem, L. D. (2015). Fouling control of a ceramic microfiltration membrane for direct sewer mining by backwashing with ozonated water. *Separation and Purification Technology*, 142:268–273.

G. Hairston Jr., N. and Fussmann, G. F. (2017). Lake ecosystems. www.els.net.

Gao, W., Liang, H., Ma, J., Han, M., lin Chen, Z., shuang Han, Z., and bai Li, G. (2011). Membrane fouling control in ultrafiltration technology for drinking water production: A review. *Desalination*, 272:1–8.

Habib, R., Asif, M. B., Iftekhar, S., Khan, Z., Gurung, K., Srivastava, V., and Sillanp a a, M. (2017). Influence of relaxation modes on membrane fouling in sub-

merged membrane bioreactor for domestic wastewater treatment. *Chemosphere*, 181:19–25.

Hofs, B., Ogier, J., Vries, D., Beerendonk, E. F., and Cornelissen, E. R. (2011). Comparison of ceramic and polymeric membrane permeability and fouling using surface water. *Separation and Purification Technology*, 79:365–374.

Huang, H., Young, T. A., and Jacangelo, J. G. (2008). Unified membrane fouling index for low pressure membrane filtration of natural waters: Principles and methodology. *Environmentalal Science and Technology*, 42:714–720.

Hudson, N., Baker, A., and Reynolds, D. (2007). Fluorescense analysis of dissolved organic matter in natural, waste and polluted waters - a review. *River Research and Applications*, 23:631–649.

Kasprzyk-Hordern, B., Ziolek, M., and Nawrocki, J. (2003). Catalytic ozonation and methods of enhancing molecular ozone reactions in water treatment. *Applied Catalysis B: Environmental*, 46:639–669.

Lieu Le, N. and Nunes, S. P. (2016). Materials and membrane technologies for water and energy sustainability. *Sustainable Materials and Technologies*, 7:1–28.

Liu, B., Qu, F., Liang, H., Gan, Z., Yu, H., Li, G., and der Bruggen, B. V. (2017). Algae-laden water treatment using ultrafiltration: Individual and combined fouling effects of cells, debris, extracellular and intracellular organic matter. *Journal of Membrane Science*, 528:178–186.

Nawrockia, J. and Kasprzyk-Hordern, B. (2010). The efficiency and mechanisms of catalytic ozonation. *Applied Catalysis B: Environmental*, 99:27–42.

NOAA (2019). Noaa, partners predict large summer harmful algal bloom for western lake erie. https://www.noaa.gov/media-release/noaa-partners-predict-large-summer-harmful-algal-bloom-for-western-lake-erie. Accessed: 2019-11-02.

Oligny, L., Bérubé, P. R., and Barbeau, B. (2016). Impact of pac fines in fouling of polymeric and ceramic low-pressure membranes for drinking water treatment. *Membranes*, 6:38–52.

O'Neil, J., Davis, T., Burford, M., and Gobler, C. (2012). The rise of harmful cyanobacteria blooms: The potential roles of eutrophication and climate change. *Harmful Algae*, 14:313–334.

Pearce, G. (2007). Introduction to membranes: Filtration for water and wastewater treatment. *Filtration+Separation*, 44:24–27.

Pick, F. R. (2016). Blooming algae: a canadian perspective on the rise of toxic cyanobacteria. *Canadian Journal of Fisheries and Aquatic Sciences*, 73:1149–1158.

Qu, F., Liang, H., Tian, J., Yu, H., Chen, Z., and Li, G. (2012a). Ultrafiltration (uf) membrane fouling caused by cyanobateria: Fouling effects of cells and extracellular organics matter (eom). *Desalination*, 293:30–37.

Qu, F., Liang, H., Wang, Z., Wang, H., Yu, H., and Li, G. (2012b). Ultrafiltration membrane fouling by extracellular organic matters (eom) of microcystis aeruginosa in stationary phase: Influences of interfacial characteristics of foulants and fouling mechanisms. *Water research*, 46:1490–1500.

Sartor, M., Schlichter, B., Gatjal, H., and Mavrov, V. (2008). Demonstration of a new hybrid process for the decentralised drinking and service water production from surface water in thailand. *Desalination*, 222:528–540.

Schlichter, B., Mavrov, V., and Chmiel, H. (2004). Study of a hybrid process combining ozonation and microfiltration/ultrafiltration for drinking water production from surface water. *Desalination*, 168:307–317.

Shi, X., Tal, G., Hankins, N. P., and Gitis, V. (2014). Fouling and cleaning of ultrafiltration membranes: A review. *Journal of Water Process Engineering*, 1:121–138.

Taylor, C. (2019). This year's algae bloom on lake erie ranks as fifth largest. https://www.monroenews.com/news/20191102/this-years-algae-bloom-on-lake-erie-ranks-as-fifth-largest. Accessed: 2019-11-02.

USEPA (2019). Responding to harmful algal blooms in wyoming and on tribal lands in epa region 8. https://www.epa.gov/region8-waterops/responding-harmful-algal-blooms-wyoming-and-tribal-lands-epa-region-8. Accessed: 2019-11-02.

Van der Bruggen, B., Vandecasteele, C., Gestel, T. V., Doyen, W., and Leysen, R. (2003). A review of pressure-driven membrane processes in wastewater treatment and drinking water production. *Environmental Progress*, 22:46–56.

Van Geluwe, S., Braeken, L., and der Bruggen, B. V. (2011). Ozone oxidation for the alleviation of membrane fouling by natural organic matter: A review. *Water Research*, 45:3551–3570.

Wei, D., Tao, Y., Zhang, Z., Liu, L., and Zhang, X. (2016). Effect of in-situ ozonation on ceramic uf membrane fouling mitigation in algal-rich water treatment. *Journal of Membrane Science*, 498:116–124.

WHO (2017). Guidelines for drinking-water quality: fourth edition incorporating the first addendum.

Xia, S., Zhou, Y., Ma, R., Xie, Y., and Chen, J. (2013). Ultrafiltration of humic acid and surface water with tubular ceramic membrane. *Desalination and Water Treatment*, 51:5319–5326.

Yu, W., Graham, N., and Liu, T. (2019). Prevention of uf membrane fouling in drinking water treatment by addition of h_2o_2 during membrane backwashing. *Water Research*, 149:394–405.

Zamyadi, A., MacLeod, S. L., Fan, Y., McQuaid, N., Dorner, S., and Sébastien Sauvé, M. P. (2012). Toxic cyanobacterial breakthrough and accumulation in drinking water plant: A monitoring and treatment challenge. *Water Research*, 46:1511–1523.

Zhang, T., Lu, J., Ma, J., and Qiang, Z. (2008). Fluorescence spectroscopic characterization of dom fractions isolated from a filtered river water after ozonation and catalytic ozonation. *Chemosphere*, 71:911–921.

Zhang, X., Guo, J., Wang, L., Hu, J., and Zhu, J. (2013). In situ ozonation to control ceramic membrane fouling in drinking water treatment. *Desalination*, 328:1–7.

Zhang, Y., Tian, J., Liang, H., Nan, J., Chen, Z., and Li, G. (2011). Chemical cleaning of fouled pvc membrane during ultrafiltration of algal-rich water. *Journal of Environmental Sciences*, 23:529–536.

Appendix A

Instrumentation

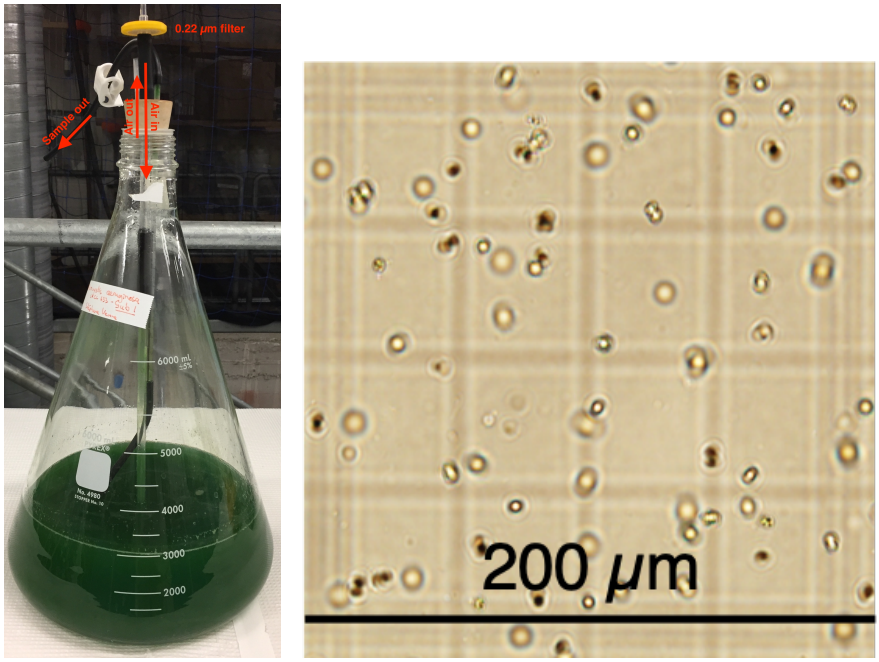

(a) (b)

Figure A.1: a) *Microcystis aeruginosa* culture in 6L Erlenmeyer growth vessel. An aquarium pump was attached to the top of the air filter. b) *M. Aeruginosa* cells under 200x magnification.

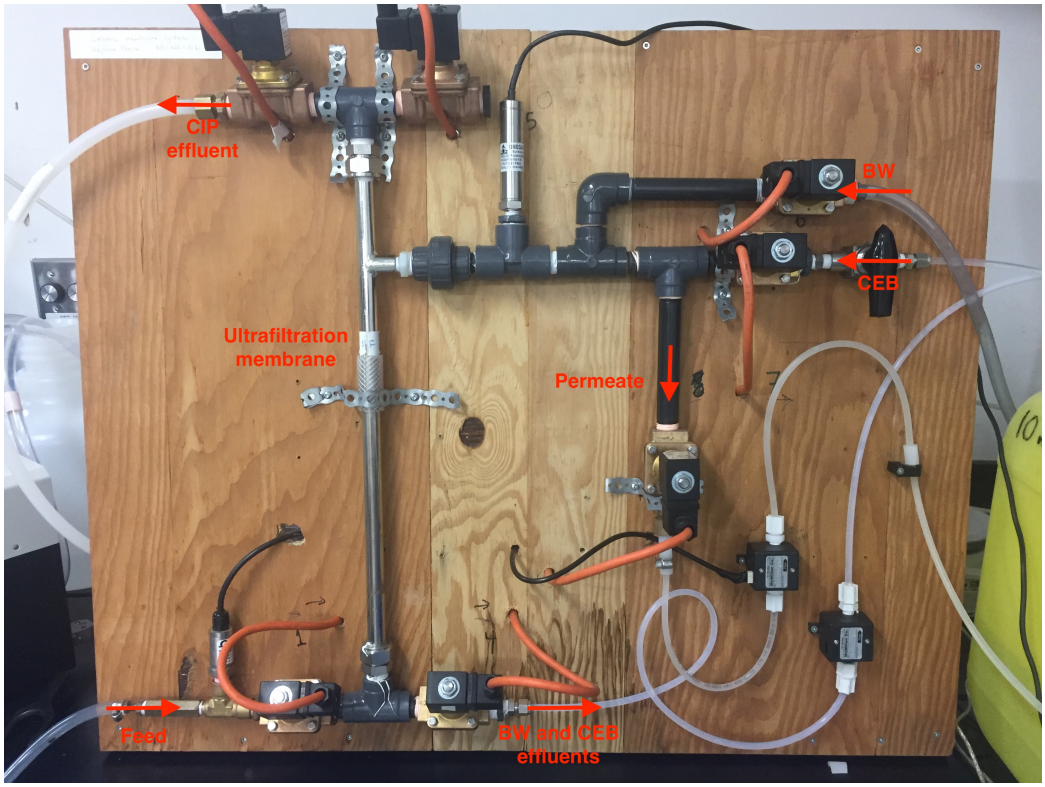

(a)

(b)

Figure A.2: a) Bench-scale ultrafiltration membrane system and b) Close-up of CEB effluent sampling location. Effluent exits the tubing at the bottom of the 45 mL glass vial, which overflows in the yellow container. Effluent is sampled from the middle of the vial with a syringe.

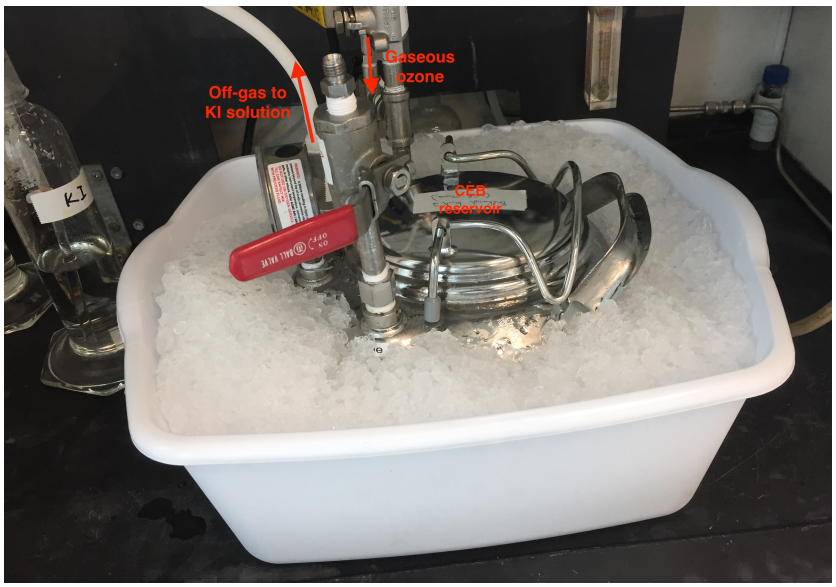

(a)

(b)

Figure A.3: a) Preparation of ozonated water for a CEB. Ozone gas is diffused through a diffuser inside of the CEB reservoir, as seen in b). The off-gas is bubbled in two potassium iodide (KI) solutions (2%) in series to quench the residual ozone.

Appendix B

Sample calculations

Cell concentration in cyanobacteria culture:

$$\begin{aligned} C &= \frac{n_{cells}}{V_{squares} * n_{squares} * f_{dilution}} \\ &= \frac{344 cells}{0.000004 mL * 4 * 1} \\ &= 2.15 \times 10^7 cells/mL \end{aligned}$$

Where C is the concentration of cyanobacteria cells in the culture, n_{cells} is the total number of cells counted, $V_{squares}$ is the volume of culture represented by a square on the hemocytometer, $n_{squares}$ is the number of squares in which cells were counted on the hemocytometer, and $f_{dilution}$ is the dilution factor of the culture used for counting.

Cyanobacteria culture volume required to obtain a concentration of 5×10^5 cells/mL in the Cyano-UW and Cyano-SW feed solutions:

$$\begin{aligned} V_{culture} &= \frac{C_{feed} * V_{feed}}{C_{culture}} \\ &= \frac{5.0 \times 10^5 cells/mL * 10L}{2.15 \times 10^7 cells/mL} \\ &= 2.15 \times 10^7 cells/mL \end{aligned}$$

Where $V_{culture}$ is the volume of culture required, V_{feed} is the volume of feed to prepare, C_{feed} is the desired cyanobacteria cell concentration of the feed, and $C_{culture}$ is the measured cyanobacteria cell concentration in the culture.

SW hardness and required calcium chloride dihydrate mass to adjust the hardness:

$$\begin{aligned} H_c &= \frac{V_2 - V_1}{V_{sample}} * 1000 mg CaCO_3/L \\ &= \frac{33.0mL - 31.1mL}{50mL} * 1000 mg CaCO_3/L \\ &= 38 mg CaCO_3/L \end{aligned}$$

$$\begin{aligned} m_{CaCl_2 \cdot 2H_2O} &= \frac{M_{CaCO_3}}{(H_f - H_c) * V} * \frac{1 mol Ca^{2+}}{1 mol CaCO_3} * \frac{1 mol CaCl_2 \cdot 2H_2O}{1 mol Ca^{2+}} * M_{CaCl_2 \cdot 2H_2O} \\ &= \frac{100090 mg/mol}{(60 - 38) mg/L * 10L} * 128980 mg/mol \\ &= 0.9 mg CaCl_2 \cdot 2H_2O \end{aligned}$$

Where H_c is the total hardness (current, before addition of calcium chloride dihydrate), V_1 and V_2 are the burette readings before and after EDTA titration respec-

tively, V_{sample} is the volume of water to titrate, $m_{CaCl_2 \cdot 2H_2O}$ is the mass of calcium chloride dihydrate to add to the feed water, M_{CaCO_3} is the molar mass of calcium carbonate, H_f is the final (desired) hardness, and $M_{CaCl_2 \cdot 2H_2O}$ is the molar mass of calcium chloride dihydrate.

Ozone concentration in solution:

$$\begin{aligned}[O_3] &= \frac{\Delta A}{f * L} * \frac{V_t}{V_s} \\ &= \frac{0.5959 - 0.3235}{0.42 * 1cm} * \frac{20.3mL}{0.3mL} \\ &= 43.9mg/L\end{aligned}$$

Where $[O_3]$ is the dissolved ozone concentration, ΔA is the difference in absorbance between sample and blank, f is the ozone absorption coeffecient, L is the path length of cuvette, V_t is the total volume (indigo solution + sample), and V_s is the sample volume.

Membrane resistance:

$$\begin{aligned}R &= \frac{\Delta P}{\mu * J} \\ &= \frac{3.69 \times 10^4 Pa}{0.00091 Pa \cdot s * 200 L/m^2 h * \frac{0.001 m^3}{1L} * \frac{1h}{3600s}} \\ &= 7.30 \times 10^{11} m^{-1}\end{aligned}$$

Where R is the total resistance, ΔP is the average trans-membrane pressure over 2.5 minutes (after a backwash or CEB), μ is the water viscosity, and J is the flux of water through the membrane.

Organic carbon left on the membrane before a CEB:

$$\begin{aligned} m_m &= m_f - m_p - m_b - m_d \\ &= ([TOC]_f * V_f) - ([TOC]_o * V_p) - \\ &\quad (([TOC]_b * V_b) - ([TOC]_f * V_m * n) - m_(([TOC]_d * V_) \\ &= (4.83mg/L * 3.82L) - (2.44mg/L * 3.82L) \\ &\quad - ((19.16mg/L * 0.179L) - (4.83mg/L * 0.014L * 4)) \\ &\quad - (7.31mg/L * 0.521L) \\ &= 2.16mg/L \end{aligned}$$

Where m_m, m_f, m_p, m_b, and m_d are the organic carbon mass left on the membrane, in the feed, in the permeate, in the backwash effluent, in the dead volume of the system (volume to flush before ozone reaches membrane during a CEB). [TOC] is the total organic concentration of the respective streams, V is the cumulative volume of the respective streams, and n in the number of hydraulic backwashes before a CEB.

Appendix C

Growth medium recipe

The stock solutions used to prepare the modified Bold's Basal Medium (3N-BBM) are presented in table C.1. The tables C.1, C.2, and C.3 were adapted from a private communication with the Canadian Phycological Culture Centre. All stock solutions were preapred in ultrapure water at room temperature. The prepared growth medium was autoclaved (15 minutes at 121°C) before use.

To prepare the F/2 vitamin stock solution as prescribed in table C.3, a concentrated stock in which the vitamin concentrations were greater by a factor of 10 was first prepared. The F/2 vitamin stock solution was then obtained by diluting 100 mL of the concentrated stock in ultrapure water.

Table C.1: Composition of stock solutions and volume required for the preparation of 3N-BMM growth media

Stock solution	Concentration (g/L)	Volume (mL/L)
KH_2PO_4	17.5	10.0
$CaCl_2{\cdot}2H_2O$	25.0	1.0
$MgSO_4{\cdot}7H_2O$	75.0	1.0
$NaNO_3$	250.0	3.0
K_2HPO_4	75.0	1.0
NaCl	25.0	1.0
$Na_2EDTA{\cdot}2H_2^*$	10.0	1.0
KOH*	6.2	
$FeSO_4{\cdot}7H_2O$**	4.98	1.0
H_2SO_4**	1***	
Trace metal solution	See table C.2	1.0
H_3BO_3	11.5	0.7
F/2 vitamin solution	See table C.3	1.0

*Prepared as one stock solution
**Prepared as one stock solution
***Expressed as mL/L instead of g/L

Table C.2: Composition of trace metal stock solution

Component	Concentration (g/L)
H_3BO_3	2.86
$MnCl_2{\cdot}4H_2O$	1.81
$ZnSO_4{\cdot}7H_2O$	0.2220
$Na_2MoO_4{\cdot}2H_2O$	0.3900
$CuSO_4{\cdot}5H_2O$	0.0790
$Co(NO_3)_2{\cdot}6H_2O$	0.0494

Table C.3: Composition of F/2 vitamin stock solution

Component	Concentration (g/L)
Vitamin B12 (Cyanocobalamin)	0.0001
Biotin	0.0001
Thiamine	0.0200